UNIVERSITY OF CALIFORNIA,
IRVINE

Hippocampal Representations of Sequences of Events: Temporal Coding and (Nonspatial) Sequence Replay in Hippocampal Ensembles

DISSERTATION

submitted in partial satisfaction of the requirements
for the degree of

DOCTOR OF PHILOSOPHY

in Biological Sciences

by

Mansi Pravin Saraf

Dissertation Committee:
Associate Professor Norbert Fortin, Chair
Professor Craig Stark
Professor Babak Shahbaba

2024

DEDICATION

To

all parents who generously devote their lives to providing education, support, and inspiration to their children

TABLE OF CONTENTS

LIST OF FIGURES

ACKNOWLEDGEMENTS

Writing this thesis has been a challenging yet rewarding journey, and I am grateful to have had the support and encouragement of many wonderful individuals. Without their help, this thesis would not have been possible.

First and foremost, I would like to express my sincere gratitude to my advisor, Prof. Norbert Fortin, for his invaluable guidance, support, and patience. I am truly grateful for the time and effort he has invested in me over the years. His insights and feedback have been crucial in shaping me as a researcher.

Next, I would like to thank my other thesis committee members: Prof. Babak Shahababa and Prof. Craig Stark for serving on my committee and providing valuable feedback on my research ideas along the way. I want to thank Prof. Babak Shahababa for guiding me in building background in statistics, which was foundational to the research presented in this thesis and also personally very rewarding. I also want to thank Prof. Craig Stark for always being available, giving me time, and guiding me through the process with patience and feedback, which was crucial in navigating the challenges of my research.

I am also indebted to my wonderful colleagues Dr. Gabriel Elias, Keiland Cooper, and other lab members of the Fortin and Shahbaba lab who have provided me with critical feedback, insightful comments, and stimulating discussions. Their encouragement and support over the last few years have been instrumental in keeping me motivated and focused on my research.

I would like to extend my deepest appreciation to my husband, Siddharth, for his strong support throughout my journey of completing this PhD thesis. His encouragement, understanding, and patience have been instrumental in my success. Finally, I would like to express my heartfelt gratitude to my parents and my sister, who have supported me throughout this journey. Their unwavering love and encouragement have been a constant source of strength and motivation. I am also incredibly grateful to the rest of my family and amazing friends. Their camaraderie, kindness, and laughter have made this long journey more manageable. Thank you all for your invaluable support and encouragement.

The text of Chapter 2 of this dissertation is a reprint of the material as it appears in "Hippocampal ensembles represent sequential relationships among an extended sequence of nonspatial events" in Nature Communications, used with permission from Springer Nature (CC BY 4.0). The co-authors listed in this publication are Babak Shahbaba, Lingge Li, Forest Agostinelli, Keiland W. Cooper, Derenik Haghverdian, Gabriel A. Elias, Pierre Baldi, and Norbert J. Fortin who directed and supervised research which forms the basis for the dissertation.

This work was supported by NIH (awards R01-MH115697, R01-DC017687, and T32-DC010775), NSF (awards CAREER IOS-1150292, DGE-1839285, and BCS- 1439267), and the Whitehall Foundation (award 2010-05-84).

VITA

Mansi Pravin Saraf

2016 B.S. in Biology, University of Utah

2024 Ph.D. in Biological Sciences, University of California, Irvine

FIELD OF STUDY

Neurobiology and Behavior

PUBLICATIONS

Shahbaba, Babak, Lingge Li, Forest Agostinelli, Mansi Saraf, Keiland W. Cooper, Derenik Haghverdian, Gabriel A. Elias, Pierre Baldi, and Norbert J. Fortin. "Hippocampal ensembles represent sequential relationships among an extended sequence of nonspatial events." *Nature communications* 13, no. 1(2022):787.

ABSTRACT OF THE DISSERTATION

Hippocampal Representations of Sequences of Events: Temporal Coding and (Nonspatial) Sequence Replay in Hippocampal Ensembles

by

Mansi Pravin Saraf

Doctor of Philosophy in Biological Sciences

University of California, Irvine, 2024

Associate Professor Norbert Fortin, Chair

The ability to temporally organize our memories is critical to daily life function and impaired in several cognitive disorders. Considerable research shows that this fundamental capacity is conserved across modalities and species, and that it critically depends on the hippocampus. However, it remains unclear *how* the hippocampus supports this capacity.

Accumulating evidence from rodent electrophysiology points to two main coding properties as potential neural mechanisms. First, ensemble activity exhibits sequential firing fields (or "time cell" activity) during individual stimuli or intervals. Although this form of temporal coding has been shown to provide significant temporal information during such task events, a direct link with the ability to remember sequences of events has yet to be established. Second, hippocampus ensemble activity has also been shown to represent sequences of spatial locations, which can be reactivated during "offline" moments such as during sharp-wave ripple events. However, it remains to be determined whether this form of sequence coding extends to nonspatial information and thus reflects a fundamental process supporting the memory for event sequences. To address these critical issues, I analyzed existing datasets in which CA1 neural activity was

recorded in rats performing a nonspatial sequence memory task, a task previously shown to have strong behavioral parallels in rats and humans and to engage comparable circuits across species.

The central aim of this thesis was to investigate temporal and sequence coding properties in hippocampus and determine their respective contributions to order memory judgments. To do so, I took advantage of this rich behavioral paradigm and applied advanced statistical tools designed to quantify these coding properties during specific task events and intervals in between them. The background and significance of my research are described in Chapter 1, my specific research aims (outlined below) are described in Chapters 2-4, and a general discussion of our findings and their implications is included in Chapter 5.

Aim 1: Determine if CA1 ensemble activity provides a temporal signal that carries event specific information and bridges across event sequences (Chapter 2). Specifically, I examined whether the temporal coding is stimulus-specific and important for correct order decisions, captures sequential relationships among stimuli through a lag effect, and bridges across sequences of stimuli. To do so, I applied a Bayesian model to quantify the temporal information contained in the hippocampal ensemble activity during discrete task events as well as across sequences of events.

Aim 2: Build statistical framework to quantify sequence replay of discrete nonspatial states during offline periods of our sequence memory task (Chapter 3). I developed a statistical framework to overcome the shortcomings of earlier models which are primarily designed to quantify the replay of continuous spatial states. Specifically, my objective was to build a framework which can detect the replay of odor sequences and determine if their content and direction conform to our predictions. To do so, I adapted the "sequenceness metric" from a human MEG study and expanded it to identify the precise order in which odors are replayed

within replay moments and make it suitable to the electrophysiological data from our sequence memory experiment.

Aim 3: Determine if nonspatial event sequences are reactivated during hippocampal replay moments and if the direction and content of the replay reflects trial-specific demands and behavior (Chapter 4). I investigated whether replay mainly reflects sequences of discrete events reflecting task critical associations and if its content and direction vary based on the interval type (temporal location in the sequence). Specifically, I tested whether replay is primarily in forward direction, involving upcoming odor sequences during rest within sequence presentation, and in reverse direction, involving odor sequences leading to sequence completion during rest at the sequence's end. To do so, I utilized the framework from chapter 3.

CHAPTER 1: BACKGROUND AND SIGNIFICANCE

In this chapter, I summarize the scientific literature relevant to my work. First, I describe the anatomy of the hippocampus to provide context for the literature. Then, I review other relevant work, including the temporal organization of memories, time cell activity, the temporal context model, and hippocampal replay. I conclude the chapter by highlighting the significance of my research.

1.1. ANATOMY OF THE HIPPOCAMPUS

Episodic memory which is the capacity to recall specific personal experiences detailing *what* happened, *when*, and *where*, involves a broad network of brain regions. This includes neocortical association areas and components of the medial temporal lobe (MTL) system which are the hippocampus as well as the adjacent entorhinal cortex, perirhinal cortex (PER) and postrhinal cortex (parahippocampal cortex in primates). The anatomical structure of the primary pathways that facilitate interactions between the neocortex and medial temporal regions, as well as the internal organization of the medial temporal areas is mainly preserved across mammalian species (98-99,101-102).

The structure of this system is characterized by projections from nearly all neocortical association areas converging onto the parahippocampal cortical areas adjacent to the hippocampus. These, in turn, project onto each subdivision within the hippocampus. Importantly, the information about the *"what"*, *"where"*, or *"when"* of individual events is not integrated into a single representation before reaching the hippocampus, suggesting that the role and anatomy of the hippocampus is crucial for episodic memory formation (3).

Briefly, the hippocampus, located in the brain's medial temporal lobe, plays a vital role in memory formation, particularly in encoding and retrieving sequences. Its complex structure is essential to its function, comprising of three main areas: the cornu ammonis (CA regions), the dentate gyrus, and the subiculum, each contributing uniquely to information flow and processing (3,100). The CA regions are further divided into CA1, CA2, CA3, and CA4, each with specific neurons and pathways. The hippocampus primarily follows the trisynaptic circuit, beginning with the entorhinal cortex, progressing to the dentate gyrus, then to CA3 and CA1, and finally reaching the subiculum. Specifically, major inputs to the hippocampus originate from the entorhinal cortex and progress to the dentate gyrus, which is the initial stage of the trisynaptics circuits, and is also essential to processing new information and for pattern separation to differential similar memories. Dentate gyrus projects to CA3 through mossy fiber connections. CA3 projects to itself, through recurrent connections, as well as to CA1, through the Schaffer collaterals. The major outputs of the hippocampus originate from CA1 (also the focus of this thesis) and the subiculum. The subiculum serves as bridge between hippocampus and other brain regions, transmitting information from CA1 to various areas, including the entorhinal cortex, thus facilitating the broader distribution of processed memory information.

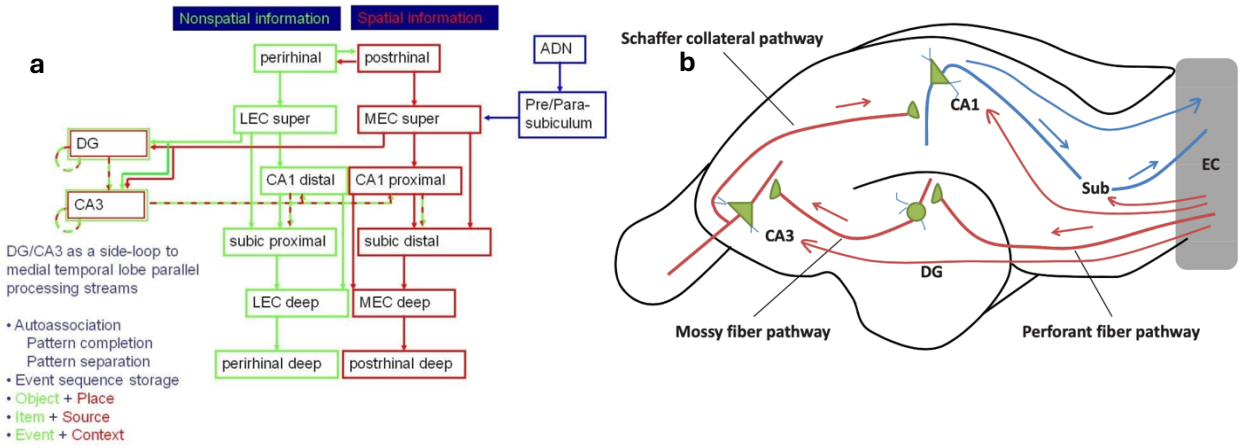

Fig 1.1. | Anatomy of the hippocampus. (a) Parallel streams of processing through the hippocampus showing pathways through which it integrates information about *what*, *when* and *where* of events. Image from Knierim et al. (149). **(b)** Input and output pathways of hippocampal formation. Entorhinal cortex (EC) is the main input to the hippocampus. EC projects to the dentate gyrus (DG) via perforant fiber pathway and provides the critical input to CA3 via mossy fiber pathway, then to CA1 by means of the Schaffer collateral pathway. Additionally, EC can also project directly to CA3, CA1 and subiculum (Sub). EC is the major output of the hippocampus. Image from Zhang et al. (150).

1.2. TEMPORAL ORGANIZATION OF MEMORY

The temporal organization of memories is a fundamental aspect of episodic memory, enabling us to arrange events in a sequential order, and recall the flow of time within our experiences (3, 20). This organization is closely related to the memory of *what-when*, where the brain encodes not only the specifics of an event (the "what") but also its temporal context (the "when"). An illustrative example of this is how an individual might remember a typical day: waking up, having breakfast, and then proceeding to work, with each event not just recalled for its sensory details but also positioned within a specific timeline. This capacity is critical to many cognitive functions, including our ability to remember the order of daily life events, plan sequences of actions to reach specific goals, and importantly, is impacted in various clinical scenarios (13-14).

Accumulating research from rodents and humans, suggests this capacity is shared across species (46), and that the hippocampus plays a critical role in supporting it (3, 15, 28, 48, 68). The evidence for this mainly comes from lesion studies in rodents and fMRI studies in humans. Specifically, in sequence memory paradigms, rats with hippocampal damage displayed normal memory for individual items but failed to recall the temporal relationships among events (15-16), suggesting hippocampus role in forming these *what-when* associations. In line with this, functional neuroimaging studies further confirm the hippocampus's significant involvement in humans during similar tasks (24, 53-54).

There has also been research to get insights into the neural mechanisms with which the hippocampus might support this ability. Importantly, previous research emphasizes the hippocampus's ability to generate sequences as vital for supporting this memory function (55-59). This is demonstrated by electrophysiological evidence suggesting that the hippocampus provides an internal representation of elapsed time, with individual neurons exhibiting robust timing signals during stimulus-free intervals, known as "time cells" (27, 28, 54), and during the presentation of event sequences (10). Moreover, the pattern of activity in hippocampal ensembles changes over time, a form of population coding that could act as a timing signal (63-64). Another line of evidence comes from sequential reactivation of hippocampal neurons corresponding to goal relevant experiences during moments of rest (38, 40-41), suggesting a sequence coding mechanism which might extend to memory of events in a sequence.

1.3. TIME CELLS

Growing evidence show presence of ‘time cells’ or “sequential firing fields” in the hippocampus. Time cells are neurons primarily found in the hippocampus or the entorhinal

cortex, that are active at specific moments in time within a temporally structured experience (10,28,71), like hippocampal "place cells" that fire when the animal is at specific location in a spatially defined environment (72-73). Time cells have been observed in different behavioral paradigms, including tasks with and without explicit memory demands (75), and in experiments in which animals are fixed in space (48,74). Importantly, the properties of these cells exhibit remarkable consistency across studies (28, 74-75), indicating a conserved temporal coding mechanism that records the elapsed time during discrete task events (28, 54, 75-76).

Strong evidence of temporal coding supported by time cells comes from studies where hippocampal neurons are shown to encode time intervals in a memory task, even as the animal stayed stationary. For instance, Pastalkova et al. (27) developed a variation of the T-maze task where the animal remained on a wheel during a pause between maze runs. Even though the animal was stationary (on the wheel), various CA1 cells activated at different times during this interval. Building on this, MacDonald et al. (28) examined hippocampal firing patterns in a nonspatial object-odor associative memory task. In this task, the animal was introduced to an object and, after a delay, approached a digging cup to determine whether to dig for a food reward based on the odor of the sand. They observed that CA1 time cells fired at distinct intervals during the pause between the object and odor presentations. Importantly, the animal was stationary during this time, indicating that the activity of time cells was not due to motion on a running wheel. Consistent with this, various studies have reported time cell activity during discrete task events including delay periods as well as stimulus presentations, suggesting their role in temporal coding during behavior (46, 48, 54, 89-94).

Studies suggests that time cells not only carry information about the timing of events but are also associated in successful learning. For example, studies found that the activity patterns of

hippocampal neurons during an odor-delayed matching-to-sample task were strongly correlated during successful trials of the same odor but less so between incorrect trials (74). This suggests that the overall activity of time cells is linked to the accurate learning and retention of sequences. In line with this, another study using calcium imaging showed that after learning, the peak activity of CA1 cells occurred at consistent times relative to tone onset, indicating that the stability of time fields depends on learning (79).

While much research on temporal coding in the hippocampus has focused on rats, some studies extended this work to non-human primates (10, 80) and humans (81). Specifically, a study recorded hippocampal activity in non-human primates during a task requiring short-term memory for the order of object pairs and showed that neurons fired at specific times during the delay between objects like the "sequential firing field activity" or the time cell activity (10). Importantly, research involving human patients with epilepsy also demonstrated that hippocampal neurons fired at successive moments during sequence learning tasks. This occurred both while subjects actively monitored a sequence and during empty gaps between events, suggesting that time cells in humans also encode temporal information vital for sequence memory (81). Collectively these evidence supports the idea that time cells play a role in temporally organizing experiences, and importantly, this is a capacity conserved across species, including humans.

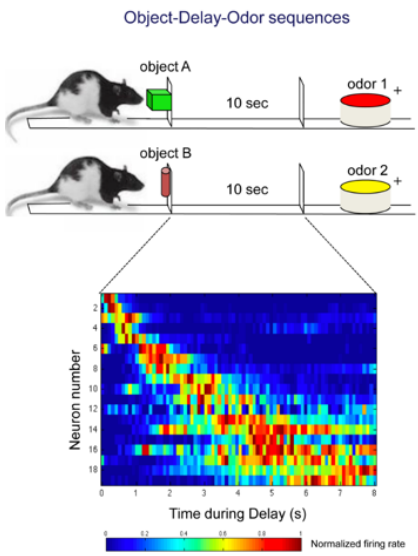

Fig 1.2. | Time cells in the hippocampus. Hippocampal neurons fire sequentially during the delay period of an object-delay-odor sequence task. The normalized firing rate of each neuron is shown in successive rows. Image from Eichenbaum et al. (148).

1.4. TEMPORAL CONTEXT MODEL

The Temporal Context Model (TCM) is a significant theoretical framework that explains how the brain encodes and retrieves memories by linking them to specific temporal contexts (82). This model posits that memories are organized based on their temporal proximity, and this organization aids in the sequential retrieval of related events. TCM emphasizes the role of context in forming associations between memories, suggesting that these associations are strengthened by the similarity in their temporal contexts. Briefly, the TCM assumes that when an event is encoded, it is associated with the current state of temporal context, which continuously changes due to ongoing experiences. Upon retrieving a memory, the associated context is reactivated, facilitating the recall of temporally adjacent memories.

The validity of TCM is supported by its ability to predict the temporal contiguity effect observed in free recall tasks, where items presented closer in time are more likely to be recalled together

(83-85). For instance, Howard et al. (83) demonstrated TCM's ability to predict the temporal contiguity effect in episodic memory using a free recall task where subjects were more likely to recall items presented closer in time. Other studies demonstrated that the TCM can adjust the internal representation of time to maintain a scale-invariant perspective (78, 86-87). This means that TCM adapts the way time is represented in the brain, ensuring that the perception and memory of time remain consistent, regardless of the actual duration or intervals between events. This capability highlights TCM's robustness in modeling how our brains encode and recall sequences of events over various temporal distances while preserving a coherent temporal context. One possible way the TCM may be reflected in neural mechanisms is through the sequential firing of time cells. Specifically, by representing sequential moments in time involving gradually changing temporal context and reflecting the sequential relationship among events, this activity could provide as a mechanism for the hippocampus to recall events based on their temporal order, thereby supporting the TCM. These studies collectively support TCM as a key framework in understanding how temporal context influences organization of events and their retrieval.

1.5. HIPPOCAMPAL REPLAY

Hippocampal replay is a phenomenon where the hippocampus reactivates sequences of neuronal activity corresponding to prior experiences or learned behaviors, during periods of awake restfulness or sleep. This neurophysiological process is linked to many fundamental cognitive processes including memory consolidation, planning, decision making, and adaptive behaviors (103, 115-118, 132).

Numerous studies investigating hippocampal replay have concentrated on sharp-wave ripple (SWR) associated replay (118). Briefly, SWRs are high-oscillation events, which happen when sharp waves, which are large amplitude negative polarity deflections (40–100 ms) in the CA1 stratum radiatum, coincide with ripples, which are brief and fast oscillatory patterns in the LFP of the CA1 pyramidal layer. This combination forms the SWR complex, which is observed in the hippocampus of various species, including humans and rodents (104, 127-129). Bulk of the research in this domain has revealed that neurons involved in SWR events are sequentially replayed, mirroring goal-related spatial trajectories that were previously experienced during behavior (41, 114, 127-128, 132).

Evidence linking hippocampal replay to cognitive processes comes mainly from spatial studies that include periods of slow wave sleep or quiet wakefulness (i.e., rest periods during behavior when the animals are not actively exploring; 105). Importantly, studies have shown that electrical interruption of SWRs (112-113, 136) or blocking them (115), and presumably replay, reduced the rate at which animals acquired a spatial memory task. Consistent with these findings, other studies have also shown that the number of goal location reactivations during replay events predicted performance, suggesting a role of replay in supporting task demands (110-111). Importantly, many studies, such as those demonstrating the coupling between SWRs and cortical up-states, support the theories that replay events facilitate stabilization and integration of memories through transfer of information from hippocampus to other cerebral regions predominantly the neocortex (118, 134-135).

Many studies have revealed distinct mechanisms within hippocampal replay and their unique contributions to cognitive tasks. Initially, research focused on sleep-based reactivation, particularly during slow-wave sleep, showing the replay of reward-relevant sequences in the

same order as initially experienced (known as forward replay; 132-133). This includes the replay of sequences of locations on a spatial trajectory in their original temporal order. Later, this phenomenon was also observed during brief periods of quiet wakefulness, which revealed further insights into replay mechanisms (38, 105-106). Specifically, Foster and Wilson (109), followed by others (103, 106, 115, 118), found that awake replay, while still compressing previous activity temporally, did not always replay sequences in the forward direction. Specifically, awake replay could also unfold in the reverse temporal sequence of the original behavior, as if the prior neural activity patterns were being replayed backward. These studies provide clear evidence that replay occurs in two directions during quiet wakefulness—forward and reverse—and only in the forward direction during slow wave sleep, suggesting their distinct contributions in supporting cognitive processes and supporting task demands (133-135).

Accumulating research investigating the role of replay content and its direction in meeting task demands, found that the distribution of forward and reverse replay during task events is distinct. Most of these studies involve rats in a spatial navigation task. Specifically, many studies revealed that when rats are distant from their goal, replay was strongly biased to encode spatial trajectories starting from the rat's current location and ending at goal location (38, 107, 121, 137, 144). In line with this, studies have shown that rats' subsequent paths closely align with the replay-encoded trajectories (105, 108, 122). Collectively these results suggest that forward replay plays a role in planning and evaluating paths leading to goals and can simulate trajectories leading to the goal and influence behavior.

On the other hand, reverse replay is more frequent when the environment or task is unfamiliar to the animal, suggesting its role in learning, and forming mental maps of new settings or tasks (103, 108, 111, 124-125). While more frequent in novel settings, reverse replay

is also observed during exploration of familiar tracks (119), indicating that it serves functions beyond the initial formation of memory. Further research studies investigating reverse replay draw insights into functions of reverse replay beyond its roles in new environments. Specifically, studies show that reverse replay events are found after path traversal on reaching reward location, suggesting their role in connecting behavior with its outcome (38, 109), and consolidating reward-related memories (38, 41, 60, 111, 121-122). In line with this, studies have found that the frequency of reverse replay increases with higher reward magnitudes, suggesting that salience signals, such as dopamine release triggered by rewards or novelty, may initiate replay expression and possibly influence its content (105, 116, 144).

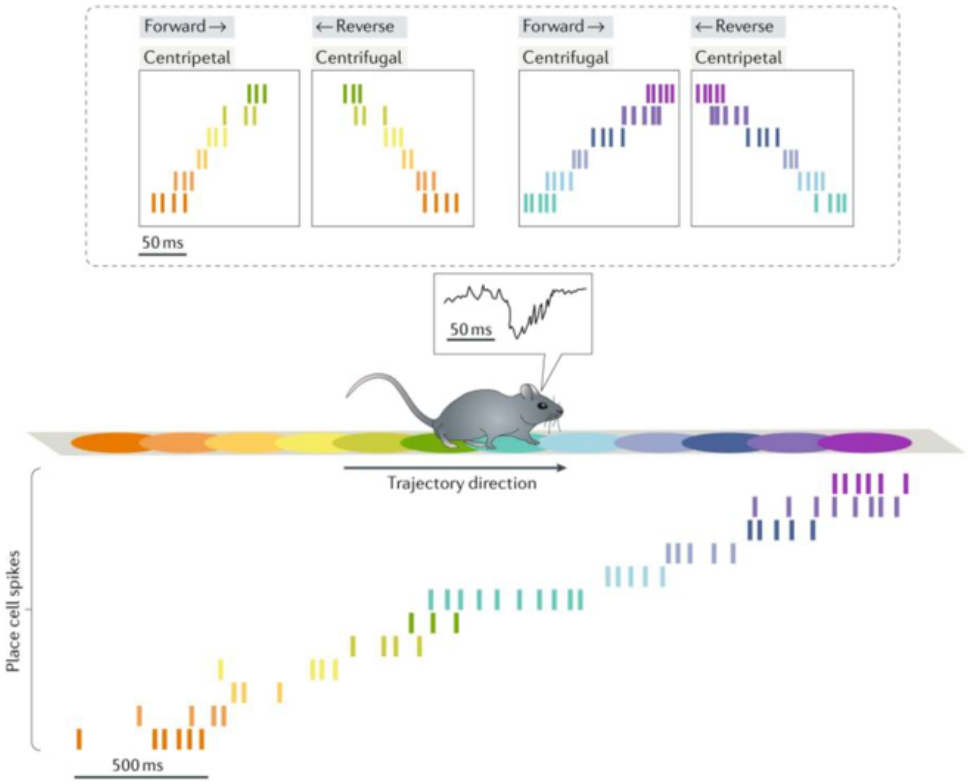

Fig 1.3. | Schematic of local replays in the forward and reverse direction. Place cells increase their firing rates as a rat traverses the cells' respective place fields on a linear track from left to right (orange to purple). When the rat pauses, immobile, at the center of the track, a SWR occurs. Place cell activity during the SWR recapitulates recent experience, firing in the same order (forward) or reverse order on a compressed timescale. Image from Joo et al. (41).

1.6. SIGNIFICANCE

1. The ability to remember temporal relationships among events is fundamental to our daily life and one of the first capacities impaired in normal aging and cognitive disorders. It is well established that the ability to temporally organize information is critical to perception, cognition, and adaptive behavior across species (1-4). Memory for temporal relationships is also an essential feature of episodic memory, as the memory for individual events includes information about the order in which they occurred during an experience (3, 5-11). Deficits in episodic memory, and in the memory for sequences of events specifically, can be detected in the early stages of several clinical conditions, including age-associated memory loss, Alzheimer's disease and other dementias (13), and following radiotherapy treatment for brain cancer (14). Despite the significance of this problem, the precise neural mechanisms underlying these cognitive impairments remain unknown, a crucial knowledge gap impeding the development of novel treatment platforms aimed at mitigating these adverse effects.

2. The hippocampus is critical to the temporal organization of memory, but its contribution and underlying mechanisms remain elusive. While our understanding of how the brain processes the spatial context of memories has advanced considerably, our understanding of their temporal organization lags far behind. Rodent studies have demonstrated that the hippocampus is necessary for temporal order memory, with corresponding findings observed in humans and nonhuman primates (18-20). In addition, fMRI research has shown hippocampal activation during encoding and retrieval of temporal information (21-24), and there is evidence that spatial patterns of activity (across voxels) in the hippocampus carry information about order or sequences (25-26). Although the involvement of this neural circuit is well established, very little

is known about its underlying neurobiological mechanisms to produce memory for sequences of events. Thus, there is a clear need for recording neural activity while animals perform a rich behavioral paradigm like ours, with precise measurements of the timing of stimuli and responses, to be able to shed light on their respective information processing dynamics.

3. Time cell coding in hippocampus can provide a temporal signal during task events, but it remains to be determined how this information supports the memory for temporal relations among events. Time cells are neurons, first demonstrated in the hippocampus (27-28) but now reported in other structures as well (29), that consistently fire at specific moments in time during task events. This activity has been demonstrated during inter-stimulus intervals as well as during stimuli presentations. While this form of activity has been shown to provide significant temporal information within such task events, it is unclear how (or if) it underlies the hippocampus' fundamental role in temporally organizing experiences. Specifically, it has yet to be determined whether this activity is linked to the ability to correctly identify the order of events, carries information about the temporal relationships among events, and bridges across individual events within a sequence. Our approach will be able to directly test these important but unresolved questions.

4. Hippocampus activity can capture sequential relationships among spatial locations during SWR-associated replay, but we do not know if this is a key coding property extending to nonspatial information. Based on its unique neural architecture, several prominent models have proposed that a fundamental function of the hippocampus is to code for sequences of inputs or events (31-37). Consistent with this view, evidence from hippocampal

recordings in rats exploring environments have revealed that hippocampal activity can reactivate representations of previously traversed or upcoming sequences of locations in a time-compressed way during SWRs (sequence replay) (38-41). However, it remains to be determined if this coding property is limited to spatial information processing, or if it extends to nonspatial memories and thus reflects a fundamental function of hippocampal circuits.

5. We need a new framework to test if hippocampal replay content extends beyond that of spatial information. Current frameworks for testing hippocampal replay are primarily suited for replaying continuous states like spatial locations (106, 138-141, 147). They also rely on the assumption that the states being replayed are well-represented by neurons with selective firing, like how place cells represent spatial locations (106). However, to investigate if replay extends to non-spatial modalities, we need a framework capable of testing replay for discrete states which will be fewer in number (as compared to spatial locations) and may not be continuous (such as daily life episodes that are temporally separate). Moreover, these discrete task events may not have as clear a representation as spatial locations do in place cells. Crucially, the framework should also be able to detect replay moments independently of SWRs, aligning with recent findings that show replay occurring outside of SWRs (137, 145-146). While there are frameworks that can detect nonspatial event replay without being tied to SWRs, these have not yet been applied to electrophysiological data and are only applicable to determine the replay of event pairs, and not sequence of 2+ events.

CHAPTER 2: DETERMINE IF CA1 ENSEMBLE ACTIVITY PROVIDES A TEMPORAL SIGNAL THAT CARRIES EVENT SPECIFIC INFORMATION AND BRIDGES ACROSS EVENT SEQUENCES

2.1. RATIONALE

Previous studies found that hippocampal ensemble activity exhibits sequential firing fields (i.e., "time cells") during the presentation of individual stimuli, delay periods and across contiguous stimuli (27-28, 30). Although this type of activity has been shown to provide a strong temporal signal within such task events (16, 24, 48, 53-54), it remains unclear whether it supports the temporal organization of events widely separated in time, a characteristic feature of our daily life experiences. To address this issue, we took advantage of our unique behavioral paradigm and extended these findings by determining whether temporal coding (time cell activity) in hippocampal neurons also captures information about the identity of individual stimuli, their positions in a sequence, and bridges across a series of stimuli presentations. Specifically, we tested the following three main hypotheses: (i) Is the temporal coding stimulus-specific and important for correct order decisions? (ii) Does the temporal coding capture sequential relationships among stimuli through a lag effect? (iii) Does the temporal coding extend beyond individual stimuli and bridge across sequences of stimuli?

2.2. APPROACH

2.2.1. DATA

I used existing spike train data from CA1 neurons from five rats as they performed the sequence memory task, specifically, during one session from the Well-Trained sequence (odors

ABCDE). Recordings were obtained from chronically implanted micro drives containing 20 independently drivable tetrodes. Action potentials from individual neurons were manually isolated offline using a combination of standard waveform features across the four channels of each tetrode (Offline Sorter, Plexon). The total number of units during session performance across five rats is 370 (rat 1 = 92, rat 2 = 79, rat 3 = 104, rat 4 = 49, rat 5 = 46). For each analysis, I only included neurons that were active (i.e., fired at least one spike) during corresponding task events of interest (e.g., presentation of each odor).

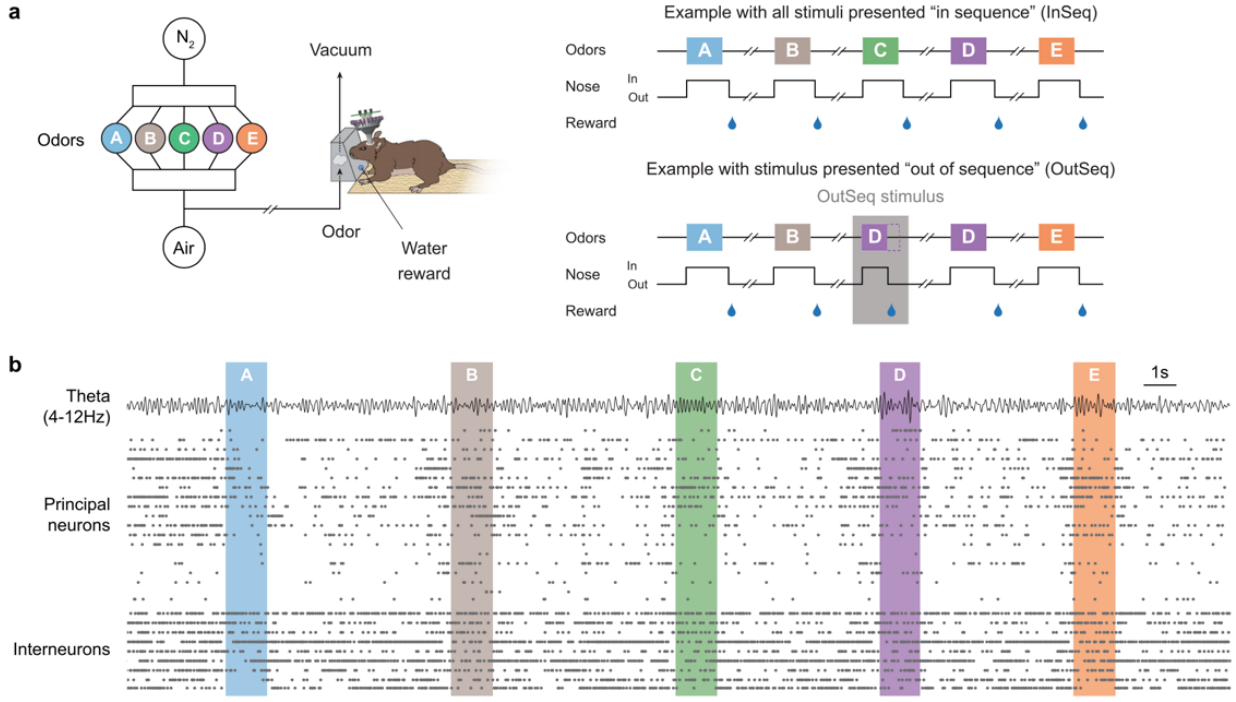

Fig. 2.1. | Neural activity was recorded from hippocampal region CA1 as animals performed a complex nonspatial sequence memory task. (a) The task involves repeated presentations of sequences of nonspatial events (odor stimuli) and requires subjects (rats) to determine whether each stimulus is presented "in sequence" (InSeq; e.g., ABC...) or "out of sequence" (OutSeq; e.g., ABD...). Using an automated odor delivery system (left), self-paced sequences of five odors (odor A = sky blue, B = brown, C = green, D = purple, E = orange) were presented in the same odor port (median interval between consecutive odors ~5 s). In each session, the same sequence was presented multiple times (right), with approximately half the presentations including all InSeq trials (top) and the other half including one OutSeq trial (bottom). Each odor presentation was initiated by a nosepoke and rats were required to correctly identify each odor as either InSeq (by holding their nosepoke response until a tone signaled the end of the odor at 1.2 s) or OutSeq (by

withdrawing their nose before the signal; <1.2 s) to receive a water reward. Incorrect InSeq/OutSeq judgments resulted in termination of the sequence. **(b)** Example ensemble activity (putative principal neurons and interneurons) and theta oscillations (bandpass: 4–12 Hz) from representative subject during one sequence presentation. Principal neurons and interneurons were separately sorted by their peak firing time in relation to the port entry triggering delivery of odor A. Figure from Shahbaba et al. (153)

2.2.2. SUMMARY OF APPROACH

First, I visualized ensemble spiking activity using peri-stimulus time histograms (PSTHs; see methods for details) sorted by peak firing latency. Then, to quantify temporal coding during specific task events, I applied a Bayesian model, commonly used to decode spatial information (62), and recently used to decode temporal information (48). Briefly, I first train the algorithm on the ensemble activity from individual bins of a task event. Then, by feeding in the ensemble activity during a specific time bin (from the testing data), the algorithm returns a probability distribution of reconstructed times corresponding to the likelihood that the test time bin occurred during each time bin used for model training. To examine temporal coding during task events, I plot these probability distributions obtained for each consecutive time bin of the testing data in the form of heat maps (Fig 2.2). A detailed description of the methods included below.

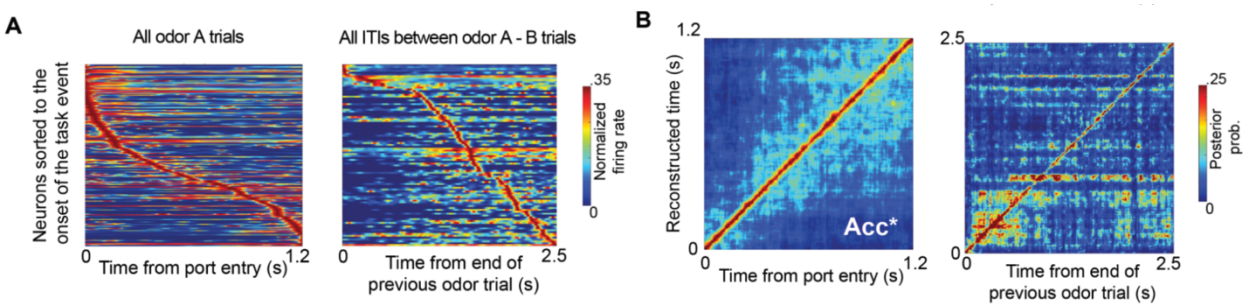

Fig. 2.2. | The Bayesian model can be used to quantify the temporal signal provided by the CA1 ensemble activity. (a) Ensemble activity during individual task events can be visualized using peri-stimulus time histograms (PSTHs; smoothed using a 150 ms gaussian; see methods) showing the normalized firing rate of all active neurons during the task events (during all odor A trials on left, and during the intervals between all odor A and odor B trials on right). Red indicates the maximum firing rate of each neuron, and blue indicates 0 Hz. **(b)** Temporal information provided by the ensemble activity in panel A quantified using the Bayesian model. Heat maps

show reconstructed time estimates obtained from each animal's PSTH and then averaged across subjects (all odor A trials on left; intervals between all odor A and odor B trials on right). Red indicates the highest probability of reconstructed time (time points along the diagonal).

2.2.3. BEHAVIOR

Our sequence memory paradigm involves repeated presentations of sequences of odors (e.g., ABCDE) presented in the same odor port (see Fig 2.1A,B and "Behavior" section in methods for details) to rats. For each odor within a sequence, subjects are required to determine whether it is presented "in sequence" (InSeq; e.g., ABC...) or "out of sequence" (OutSeq; e.g., ABD...) to receive a water reward. Importantly, this InSeq/OutSeq judgment is performed on a trial-by-trial basis (each trial corresponds to the presentation of one odor), such that each correctly identified odor presentation is followed by a reward. An incorrect response results in early termination of the sequence.

Five naïve rats (male Long-Evans, ~350 g at the beginning of the experiment) were trained to nosepoke and reliably hold for 1.2 s in the odor port for water reward. Odor sequences of increasing length were then introduced in successive stages (A, AB, ABC, ABCD, and ABCDE) upon reaching behavioral criterion of 80% correct over three sessions per training stage. In each stage, rats were trained to correctly identify each presented item as either InSeq (by holding their nosepoke response for at least 1.2 s to receive a water reward) or OutSeq (by withdrawing their nose before 1.2 s to receive a reward). Note that OutSeq items could be presented in any sequence position except the first (i.e., sequences always began with odor A, though odor A could also be presented later in the sequence as an OutSeq item). After reaching criterion performance on the five-item sequence (> 80% correct on both InSeq and OutSeq items), rats underwent surgery for microdrive implantation. Over a few weeks, tetrodes were gradually lowered into the region of interest (pyramidal cell layer of the dorsal CA1 region).

Neural activity (spikes and local field potentials; LFP; Fig 2.1C) was then recorded as animals performed the task. Importantly, only one sequence was used during training (ABCDE; same odors and order across rats) and the same sequence was used in the recorded sessions analyzed in this thesis (i.e., Well-Trained sequence session). In addition to this session, recordings were obtained from two other sessions during which the animals were presented with a new sequence (odors VWXYZ; "Novel 1" and "Novel 2" sessions).

2.2.4. PERI-STIMULUS TIME HISTOGRAMS (PSTHs) AND CORRELATION ANALYSIS TO QUANTIFY THE SIMILARITY OF PSTHs.

The activity of individual neurons during odor presentations was visualized using peri-stimulus time histograms (PSTHs; data displayed are from a single session). Each row represents the normalized firing rate from a single neuron across trials of a specific type, normalized to its peak firing rate. More precisely, for each neuron, the activity was binned into 1ms bins, smoothed across bins using a gaussian filter (150ms for individual odor PSTHs in Fig 2.3A, 250ms for full sequence PSTHs in Fig 2.6A), then collapsed across trials to obtain the mean firing rate per bin, and finally normalized to its peak rate within the row. PSTHs for individual odor presentations (e.g., Fig 2.3A) aggregated neurons across all subjects to easily visualize the activity from all active neurons. However, to be conservative, PSTHs for full sequences (e.g., Fig 2.6A) only displayed neurons from a single subject to acknowledge potential differences in sampling or in the pacing of trials across subjects. For each PSTH, neurons that did not fire in any of the corresponding trials were excluded (though such neurons may be included in another PSTH).

The similarity among odor PSTHs was quantified using a simple correlational approach (Fig 2.4A). First, to balance the sampling, we used the same number of trials for each odor type (first 14 trials for odors A, B, C, and D; 56 trials in total). Then, we essentially produced a PSTH for each trial (neurons aggregated across subjects; firing rate in 1ms bins, gaussian smoothed and normalized) and correlated all pairs of trial-specific PSTHs (within and across odors). Correlation coefficients (r) for the different combinations of trial types (AvsA, AvsB, AvsC, etc.) were statistically compared using one-way ANOVAs. Dunnett's post hoc tests were then used to directly compare "same odor" vs "different odor" pairs (e.g., comparing AvsA with AvsB, AvsC, and AvsD) while controlling for the number of comparisons performed. Statistical significance was determined using $P < 0.05$.

2.2.5. BAYESIAN RECONSTRUCTED TIME MODEL

By assuming the ensemble spiking activity has a Poisson distribution and the spiking activity of each neuron is independent, we can use the spiking activity in a specific time window (actual time) to calculate the probability of time (reconstructed time):

$$\begin{aligned} P(\text{time}|\text{spikes, odor}) &= \frac{P(\text{spikes}|\text{time,odor}) \cdot P(\text{time}|\text{odor})}{P(\text{spikes}|\text{odor})} \\ &= C \cdot P(\text{time}|\text{odor}) \prod_{i=1}^{N} \frac{[\tau f_i(\text{time,odor})]^{n_i}}{n_i!} \exp[-\tau \sum_{i=1}^{N} f_i(\text{time,odor})] \end{aligned}$$

In Fig 2.6 B, we use P(time, odor|spikes) instead. Here, τ is the length of the time window (50 ms with step size of 5 ms in Fig 2.3B; 1500 ms with step size of 150 ms in Fig 2.6B), fi(time, odor) is the mean firing rate of the i-th unit in the time window, ni is the number of spikes occurring in the time window, odor refers to the treatment of individual odors (odors ABCD in Fig 2.2B; odors ABCDE in Fig 2.6B), C is a normalization factor to make the probability

distribution for each time window (actual time) sum up to 1, and assuming time is uniformly distributed given each odor, P(time|odor) is a constant since all InSeq trials have the same duration.

Unless otherwise noted, the model was trained using a balanced subset of sequence presentations in which all odors were InSeq, consecutively presented, and correctly identified (using a leave-one-out cross-validation approach). Plots of reconstructed time show, for each time window (actual time), the resulting probability distribution of reconstructed time averaged across subjects (red indicating max probability, blue indicating 0). Accuracy of reconstructed time was determined by quantifying the degree of relationship between actual time and reconstructed time estimates. To do so, for each trial, we calculated the correlation across rows and columns of the same index (one correlation value per row-column pair) and the mean of these correlation values represented the accuracy of reconstructed time on that specific trial. Chance levels were determined by calculating the mean reconstructed time accuracy across 1,000 random permutations of the time factor in the fi (time, odor) matrix. Statistical comparisons with chance levels were performed using one-sample t-tests (two-tailed) with statistical significance determined using $P < 0.05$.

2.2.6. COMPARISON OF TEMPORAL CODING BETWEEN CORRECT AND INCORRECT TRIALS

Comparisons between correct and incorrect trials focused on OutSeq trials because of the small number of errors observed on InSeq trials. More specifically, the model was trained on the full sequence of InSeq odors but tested on the 250-ms preceding port entry on OutSeq trials (to avoid the confounding influence of the OutSeq odor presentation). Only OutSeq trials in sequence

positions 2 to 4 were included to avoid edge effects and maximize alignment across trial types. OutSeq reconstructed time accuracy was quantified through comparison with the corresponding decoding on InSeq trials (which served as expected values). More specifically, we used a Kullback-Leibler (KL) divergence analysis to compare the shape of the probability distribution from each OutSeq trial with that of the mean probability distribution from InSeq trials. Statistical comparisons used nonparametric Kolmogorov-Smirnov tests to account for potential non-normality in the distribution of KL divergence values, though the same pattern of results was observed with parametric tests. Statistical significance was determined using $P < 0.05$.

2.3. RESULTS

2.2.1. TEMPORAL CODING IS STIMULUS-SPECIFIC AND IMPORTANT FOR CORRECT ORDER DECISIONS.

Consistent with previous reports (27-28, 30), hippocampal activity showed sequences of firing fields (“time cell" activity) during stimulus presentations and the intervals separating them. We observed strong temporal organization in the PSTHs during such task events which was associated with significant reconstructed time accuracy obtained by the Bayesian model (i.e., the degree of correspondence between actual and predicted time across trials; see methods).

We extended these findings by showing that temporal information contained within the time cell activity is stimulus-specific (Fig 2.3A). For each odor type, a strong temporal organization was observed when neurons were sorted by their peak firing latency relative to the onset of that odor, whereas this temporal organization was significantly reduced when the same sorting of neurons was examined during other odors. We quantified this in two ways: (i) by

comparing the similarity of PSTHs across odor types using a correlation analysis, and (ii) by applying the Bayesian model to quantify the temporal organization across odor types.

Using the correlation analysis, we found that the PSTHs were highly correlated across trials of the same odor type (PSTHs along the diagonal in Fig 2.3A; $r_{OdorA} = 0.7797$, $r_{OdorB} = 0.7773$, $r_{OdorC} = 0.7632$, and $r_{OdorD} = 0.7631$), and were significantly less correlated to trials of another odor type (other PSTHs in same row, which keep the neuron sorting constant). To compare correlation coefficients across different trial types in a row we used one-way ANOVAs and Dunnett's post hoc tests (Fig 2.4A). Specifically, we found that the pairwise correlations between each odor A trial and each other A, B, C, or D trial were significantly different across trial types ($F(3, 52) = 336.9$, $P < 0.0001$), with correlations across trials of the same type being significantly higher than the others (AvsA was significantly higher than AvsB, AvsC, or AvsD; Dunnett's posthoc tests P values < 0.05). Importantly, the same pattern of results were obtained for odor B (B vs A,B,C, or D: $F(3, 52) = 334.4$, $P < 0.0001$), odor C (C vs A,B,C, or D: $F(3, 52) = 258.2$), and odor D (D vs A, B, C, or D: $F(3, 52) = 237.9$).

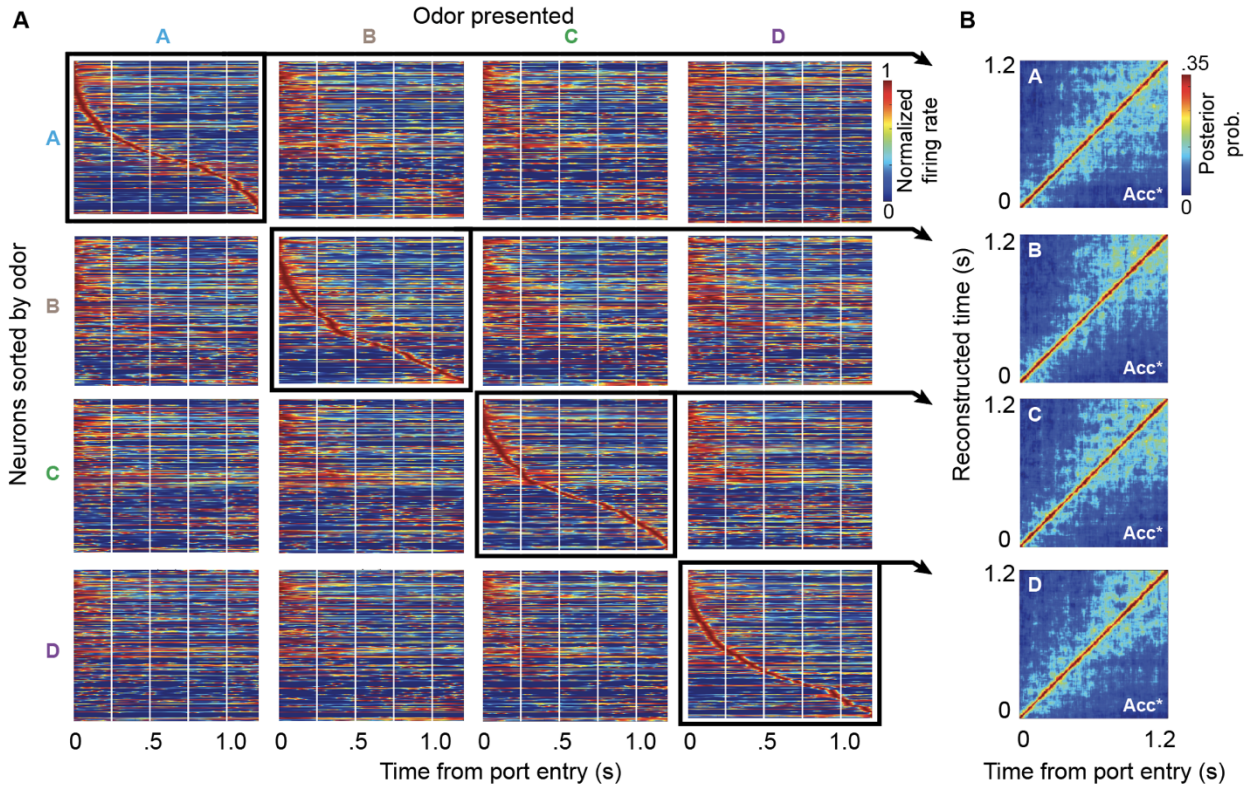

Fig. 2.3. | CA1 ensembles display sequences of firing fields ("time fields") during all stimulus presentations, which vary by the associated stimulus, and also provide a strong temporal signal during such task events. (**a**) Stimulus specificity in sequential firing fields. Each PSTH (smoothed using 150 ms gaussian) shows the normalized firing rate of all active neurons during presentation of a specific odor type (InSeq trials only; 267 active neurons for odor A, 192 for B, 209 for C, and 223 for D; neurons collapsed across five subjects, one session per subject). To visualize how sequential firing fields varied across odor types, PSTHs are shown for each odor presented (in columns), with neurons sorted by their time of peak firing relative to the onset of each odor (in rows). (**b**) Accuracy of reconstructed time for each odor type was above chance levels. Plots show reconstructed time estimates obtained from each animal's PSTH (correctly sorted for each odor, i.e., diagonal of panel A) and averaged across subjects.

Similarly, using the Bayesian model, we found that accuracy of reconstructed time was significantly higher when model training and decoding was performed on trials of the same type (e.g., train and decode using different subsets of odor A trials) than across trial types (e.g., train on odor A trials and decode B, C, or D trials; Fig 2.4B). Specifically, an ANOVA showed that, when the model was trained using odor A trials, its reconstructed time accuracy significantly varied when applied to odor A, B, C, or D trials ($F(3, 216) = 113.1$, $P < 0.0001$), with the highest

accuracy observed when we decoded the same trial type as in model training (Dunnett's posthoc tests P values < 0.0001). Importantly, a similar pattern of results was obtained when the model was trained using odor B trials ($F(3, 216) = 85.33$, $P < 0.0001$; Dunnett's posthoc tests P values < 0.0001), odor C trials ($F(3, 216) = 88.77$, $P < 0.0001$; Dunnett's posthoc tests P values < 0.0001), and odor D trials ($F(3, 216) = 71.27$, $P < 0.0001$; Dunnett's posthoc tests P values < 0.0001). Together, these findings suggest the temporal organization is stimulus-specific through correlation analysis as well as through a Bayesian model.

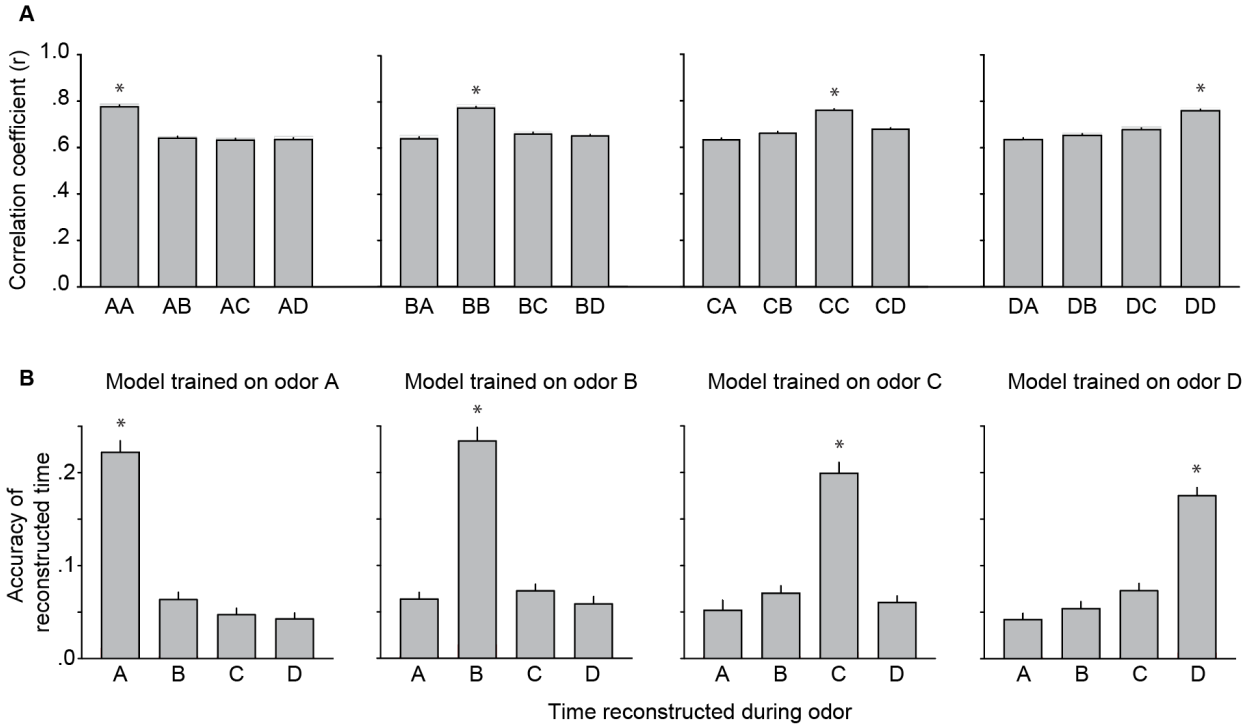

Fig. 2.4. | Stimulus specificity of sequential firing fields. (**a**) Mean correlation of PSTHs across trials of each odor type. An ANOVA showed that the pairwise correlations between trials of the same odor type and trial of different odors were significantly different across trial types, with correlations across trials of the same type being significantly higher than the others (**b**) Analysis of reconstructed time across trial types, with chance levels shown in red. An ANOVA showed that, when the model training and decoding was performed on trials of the same type, its reconstructed time accuracy significantly varied when applied to other trial types, with the highest accuracy observed when decoding the same trial type as in model training.

Finally, we determined whether this temporal signal was important for making correct order decisions. We tested this using OutSeq trials for adequate sampling of correct and incorrect responses (see methods for more details). Specifically, we used a time window which did not have any odor information (i.e., 250 ms window before port entry) as the odor type during the OutSeq trials differed. We report that the reconstructed time accuracy was significantly higher before correct responses than incorrect responses (Kolmogorov-Smirnov $D = 0.3232$, $P = 0.0149$), suggesting this form of activity supports order memory decisions.

2.2.2. TEMPORAL CODING CAPTURE SEQUENTIAL RELATIONSHIPS AMONG STIMULI THROUGH A LAG EFFECT.

Here we expanded our analysis from Aim 1a to test whether temporal coding accuracy varies as a function of the temporal distance among odor presentations (in terms of sequence positions). To do so, we calculated the reconstructed time accuracy by training the Bayesian model on spiking activity during a given odor type, and then, by testing it on all odor types organized by lag (see details in methods). We observed that, consistent with the temporal context model55-56, reconstructed time accuracy varied by lag ($F(6, 873) = 166.9$, $P < 0.0001$; Fig 2.5). It was highest for lags of 0 (i.e., train and decode using different subsets of trials from same odor type; all Dunnett's post hoc tests $P < 0.05$) and showed a significant linear decline across lags of 1, 2, and 3 in the positive direction (e.g., train on B, decode C, D, or E; $F(1, 327) = 12.93$, $P = 0.0004$) and negative direction (e.g., train on D, decode C, B, or A; $F(1, 327) = 12.20$, $P = 0.0005$). It is also important to note that reconstructed time accuracy was significantly above chance levels across all lags (Fig 2.5; all one-sample t-tests $P < 0.05$; chance level determined by permutations). Together, these results suggest that the temporal organization is partially shared

between stimuli and varies as a function of lag, such that the temporal distance between stimuli (in terms of sequence position) is reflected by the degree of dissimilarity of their neural activity.

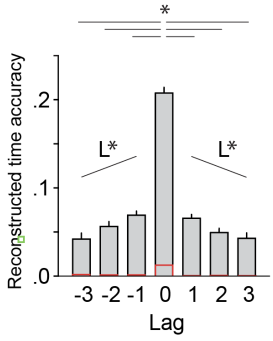

Fig. 2.5. | Temporal coding of CA1 ensembles reflect sequential relationships among stimuli through a temporal lag effect. Accuracy of reconstructed time varied by the lag between the odor type used to train the model and the odor type in which time was reconstructed (e.g., when the model was trained on odor B trials, decoding time during odor B, C, D or E trials represented lags of 0, 1, 2, or 3, respectively). Permuted chance levels for each respective lag is shown in red.

2.2.3. TEMPORAL CODING EXTENDS BEYOND INDIVIDUAL STIMULI AND BRIDGE ACROSS SEQUENCES OF STIMULI.

To determine if this temporal organization extended beyond individual stimuli and intervals, we examined the ensemble activity across the sequence of odors. Similar to our approach in Aim 1a, we used PSTHs to visualize the ensemble activity across series of stimuli and used the Bayesian model to quantify its temporal coding. Despite the variable time at which odors were presented (the task is self-paced so the time between odor presentations varied across sequences and animals), we observed substantial sequential organization of firing fields across the whole sequence (Fig 2.6A). This activity was also associated with significant reconstructed time accuracy for each animal ($t(11) = 7.043$, $t(6) = 4.730$, $t(13) = 7.941$, $t(11) = 6.174$, $t(9) = 7.398$; all P values < 0.01; same pattern of results observed using shorter and longer time bins and when collapsed across subjects; Fig 2.7). These results suggest that hippocampal ensemble activity provides significant temporal information unfolding over several seconds, and by bridging across events in the sequence. This further shows, for the first time, that the temporal signal may support our ability to temporally organize our daily life experiences.

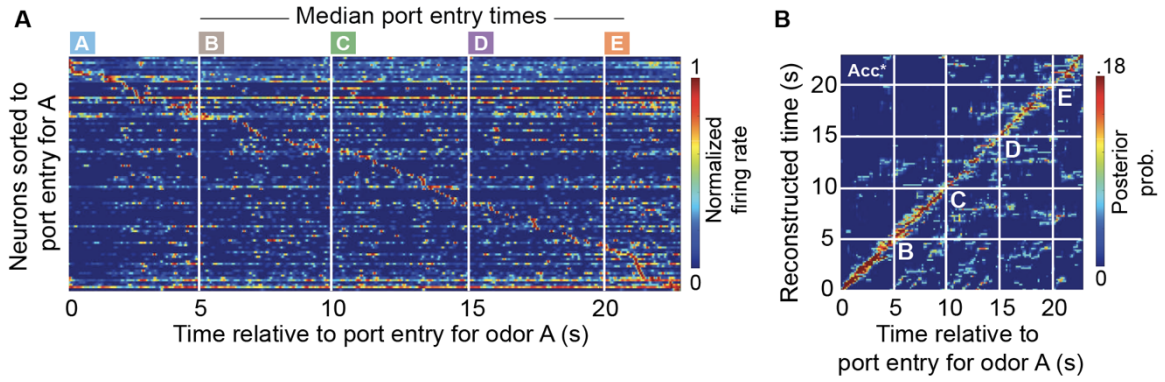

Fig. 2.6. | The temporal information provided by CA1 "time fields" extends across event sequences. (a) The sequential organization of firing fields extended across the full sequence of odors. Since the time between odor presentations varied across sequences and subjects (the task is self-paced), the PSTH (250 ms gaussian) shows data from a single subject and the median onset of odors B, C, and D across sequences. **(b)** Accuracy of reconstructed time across the sequence of odors (PSTH from panel A) was above chance levels

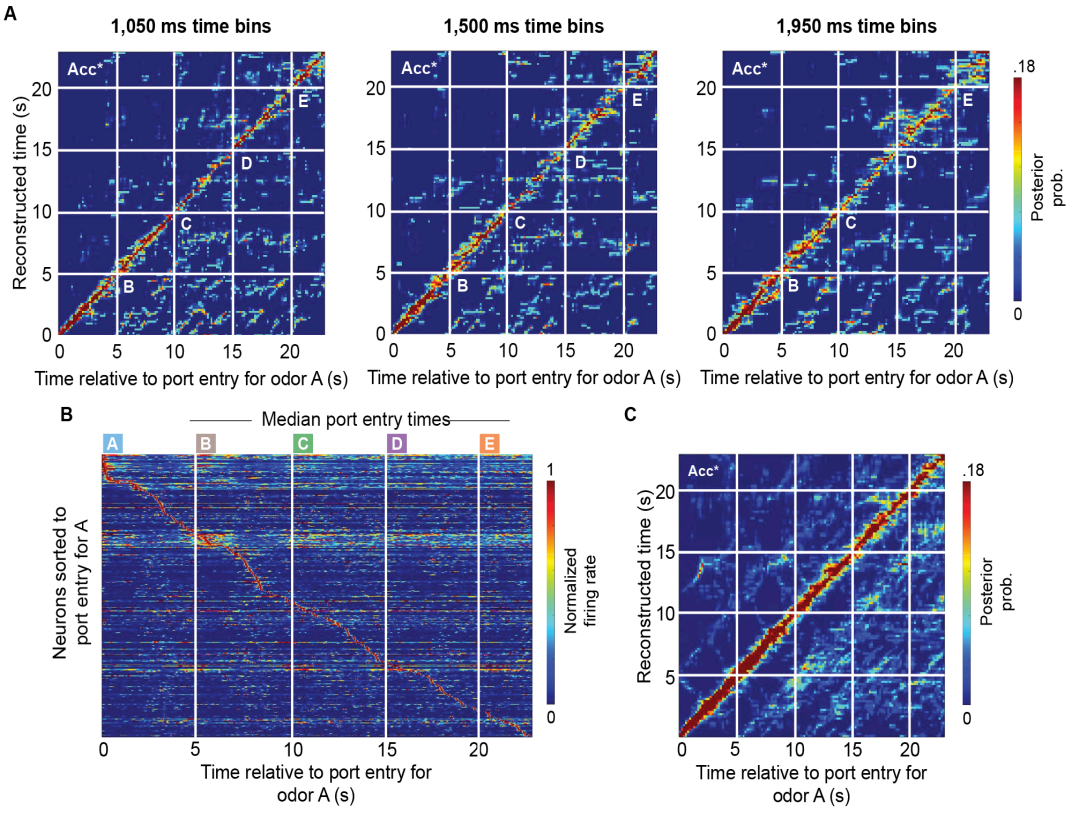

Fig. 2.7. | Temporal coding accuracy across event sequences showed the same pattern when using different time bins and averaging across animals. (a) Reconstructed accuracy was comparable using shorter ad longer time bins. Data from example subject from Fig 2.6 B are shown in the middle panel for comparison. The same analyses were then performed using shorter

time bins (left; 1,050 ms with step size of 150 ms) and longer time bins (right; 1,950 ms, with step size of 150 ms). **(b-c)** Data averaged across subjects shows the same temporal organization observed in individual subjects. Even with differences in the timing of odors across subjects (the task is self-paced), averaging across subjects revealed a strong sequential organization of firing fields and temporal coding.

2.4 DISCUSSION

In this study, we leveraged complex behavioral and statistical approaches to discover forms of sequential organization in hippocampal ensemble activity supporting the memory for sequences of events, a capacity known to critically depend on the hippocampus. We report that CA1 ensembles are organized in sequences of firing fields during individual task events. We also found that this form of temporal organization is stimulus-specific and provides strong temporal coding during these discrete nonspatial events distributed throughout the task. Interestingly, we observed that temporal coding reflects sequential relationship among stimuli through a temporal lag effect, is linked with correct order memory judgements, and importantly, also bridges across sequences of stimuli unfolding over several seconds. Collectively, these findings suggest a mechanism by which time cell activity can support memory for order of events in a sequence.

Sequential firing fields (time cells) have previously been reported during individual stimulus presentations, intervals separating them, and across contiguous stimuli and responses (27-28, 30). Considerable evidence indicates this form of coding can provide a strong temporal signal within such task events (48, 54). Here we offer direct evidence that hippocampal sequential firing fields provide significant temporal information across a sequence of discontiguous events unfolding over several seconds, and that this form of coding is important to correctly remember the order of events. These findings lend support to theoretical models proposing that this form of coding supports our ability to organize our experiences in time (10, 47,

82, 86) a characteristic feature of episodic memory (3, 10, 62, 77). Considering recent evidence that the lateral entorhinal cortex, a region with a strong anatomical and functional relationship with the hippocampus, provides a robust temporal signal across a longer timescale (several minutes; 61, 69) our results suggest that different aspects of the temporal context of episodic memories may be represented across medial temporal lobe structures.

Our unique behavioral and analytical approaches allowed us to extend previous demonstrations of conjunctive or stimulus-specific odor coding in hippocampal neurons, including individual neurons responding to a specific odor in a specific sequence position (60) or to a specific moment in time during a specific stimulus. Here we extend these previous findings by discovering that the representations of individual stimuli also contain information about their sequential relationships. In fact, we demonstrate a temporal lag effect in which the temporal distance between stimuli (in terms of sequence position) was reflected by the degree of dissimilarity of their neural activity, an effect that was observed using different metrics (temporal coding accuracy in Fig 2.2C, distance between clusters in the low-dimensional representation of the neural activity in Fig 2.3B). This effect provides a potential neural mechanism for our ability to judge the relative temporal distance and order of discrete experiences that is consistent with computational models of the representations of the temporal context of events (47, 82). We also provide a significant extension to our previous demonstration of individual neurons compatible with the view that the hippocampus plays a key role in representing task-related schemas (70), in this case, the sequential relationships among those events, to guide behavioral decisions.

CHAPTER 3: STATISTICAL FRAMEWORK TO QUANTIFY SEQUENCE REPLAY OF DISCRETE NONSPATIAL STATES DURING OFFLINE PERIODS

3.1. RATIONALE

Previous research has significantly advanced our understanding of hippocampal replay in spatial navigation tasks and its link to key cognitive functions (103, 115-118, 132). These studies highlight the essential role of hippocampal replay in consolidating spatial memories and navigating environments, mainly through the replay of spatial trajectories by place cells. They typically use the Bayesian decoding algorithm (described in chapter 2; 106, 148) and various GLM frameworks (138-139) to identify the replay content and direction. However, these methods require the replayed content to involve multiple continuous states (like spatial locations on a trajectory) and are not suitable to quantify other types of replayed content (more details on this in chapter 4). Notably, most of these methods (with some exceptions in the more recent state space models; 140-141) concentrate on SWRs to study replay and assume the onset of SWRs as the onset of the replay. This view is challenged by recent findings that show SWR detection depends on the number of recorded neurons and non-standardized thresholds, and that replay moments do not always align with SWRs (106, 137, 142-143). To address these limitations, in this chapter I developed a statistical framework that can identify replay moments during quiet wakefulness independent of SWRs and determined whether the replayed content can include sequences of discrete, temporally separated states that are fewer in number than the continuous spatial states of a trajectory.

3.2. APPROACH

3.2.1. DATA

In this chapter we utilized the same dataset used in chapter 2 and focused our analysis on ensemble activity during specific task events. We focused on InSeq stimuli presentations to train our model and on intervals between them to identify replay moments (total number of 226 odor A trials, 147 odor B trials, 130 odor C trials, 122 odor D trials, 151 odor E trials across animal; built separate classifier for each animal). Specifically, we focused on 6 different interval types, with 4 interval types during sequence presentation (i.e., before odor E; average duration of odor A intervals is 4.8 secs, 4.5. secs for odor B, 4.3. secs for odor C, 4.6. for odor D), and 2 after sequence ends (i.e., after odor E near the odor port, and at the back of the maze; 3.6 secs and 5.6. secs respectively).

3.2.2. SUMMARY OF APPROACH.

In this section, I provide an overview of our statistical framework. In the following section I explain each step of the framework in detail.

Quantifying sequence replay of discrete or discontiguous events requires a different approach than the traditional Bayesian decoding methods used to decode the replay of spatial trajectories. Spatial replay analyses can take advantage of the large set of possible states (all the possible locations in the environment) and of the fact that trajectories involve continuous series of adjacent states (locations) to constrain the definition of replay moments. Instead, our statistical framework is based on time-lagged regressions and adapted from a "sequenceness" metric initially developed for a human MEG study (90-91). In its original form this metric can identify replay moments involving event pairs of interest but is unable to quantify the replay of two or

more events and their exact temporal sequence. To address our specific questions and test our sequence replay predictions, we expanded the metric so it can identify replay moments involving significant replay of odor sequences (comprising two or more odors) and identify the precise order in which the odors are replayed.

As shown in Figure 3.1, our approach involves a series of steps aimed at quantifying the relationship between the decoded probability of two distinct states (stimuli) in successive 25-ms bins using beta coefficients (e.g., βAB; the correlation between the probability of stimulus A in bin(i) and of stimulus bin(i +1)). For each β, we built the distribution of all observed values across all bins and identify statistically significant moments, in this case moments in which the observed value is at least 3 standard deviations above the mean. To capture longer sequences, we repeated this process to calculate "consecutive βs" and generate their distribution across all bins. Consecutive βs (e.g., βABCDE represent a specific pattern of individual βs over successive 25-ms bins (i.e., βAB at bin(i) + βBC at bin(i +1) + βCD at bin(i +2) + βDE at bin(i+3). Finally, we evaluated the distribution of significant βs (individual and consecutive) across intervals against the hypothesis. Note that we focused the presentation of the results on consecutive βs (e.g., βABCDE) but that we also examined the distribution of the corresponding individual βs (βAB, βBC, βCD, βDE), as they may capture replay moments that did not meet the relatively stringent magnitude and timing requirements of the consecutive βs.

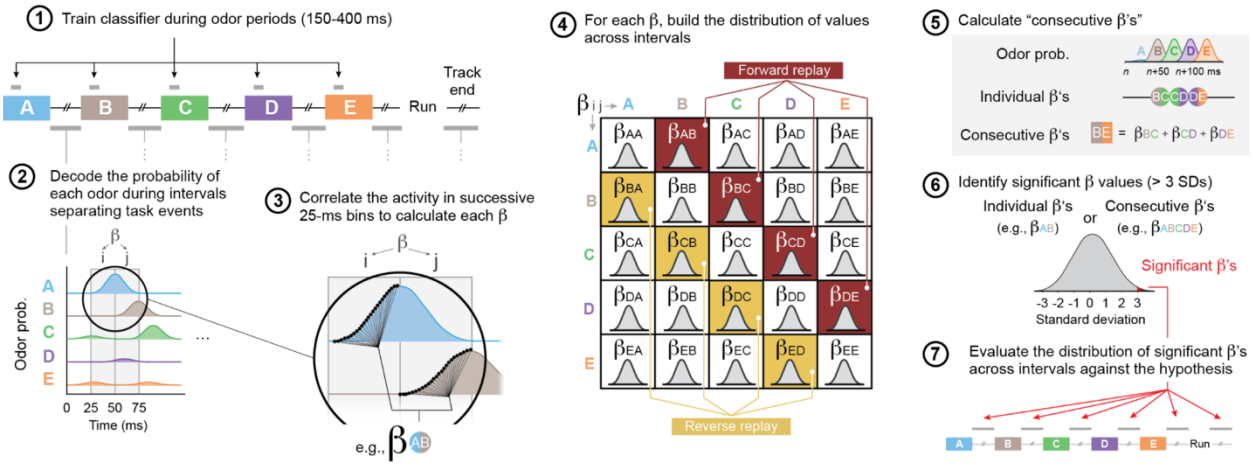

Fig 3.1. | Schematic illustrating the approach to quantify sequence replay moments. Steps 1-7 illustrate an overview of the statistical framework used to quantify replay of sequences of discontiguous states in the ensemble activity.

3.3.3. DETAILED EXPLANATION ON THE STEPS OF OUR STATISTICAL FRAMEWORK

Before going into each step of the framework in detail as illustrated in Fig 3.1, I first describe how we processed the ensemble data. We standardized the ensemble activity across intervals, which is necessary to obtain standardized regression coefficients (βs), utilized in the later stages of the framework. Specifically, we calculated the z-score activity of each neuron at every time point *t* across all intervals using the following calculation.

$$Z_{ni_t} = \frac{X_{ni_t} - \mu_{ni}}{\sigma_{ni}}$$

here, X_{nit} is the spiking activity of neuron *n* during a moment in time *t* in interval *i*, μ_{ni} is the mean activity of neuron *n* across all intervals of type *i* (e.g., all intervals between odors A and B) and σ_{ni} is the standard deviation of the activity of neuron *n* across all intervals of type *i*. I standardize the activity during odor presentations in the similarly.

Step 1: Training classifier during odor periods

We built a multinomial classifier to identify odor identity using the CA1 ensemble activity. The classifier was trained on the standardized ensemble activity from 6 distinct states (5 odor states, and a null state). Standardized ensemble activity from 300-500 ms from port entry was chosen to represent each odor type, and from a 200 ms "run period" to represent the null state. The run period occurs during interval after odor E, when the animals run to back of the maze for reward. 300-500 ms period was chosen, as this window yielded highest odor classification accuracy results across animals. Accuracy was tested using 25ms sliding windows across the odor presentation period. Since not every neuron's activity is associated with odor presentations or the null state, the LASSO model eliminated neurons that don't contribute to the odor decoding by setting their corresponding regression parameter to zero.

Step 2: Obtaining odor probabilities

This step is necessary to decode the probability of each odor during intervals separating task events. Specifically, once the multinomial classifier was built, we applied it on the ensemble activity from the intervals to obtain probability time series for each odor (odor probabilities). Odor probability values were obtained for every 25 ms window (sliding over every 1 ms) within the interval. The following steps and the results section explain why 25 ms windows (3.4.3) were chosen. The null state was incorporated only for constructing the multinomial classifier, ensuring that the odor probabilities do not aggregate to 1 (additional explanation in 3.4.2). As a result, the following steps do not use the null state.

Step 3: Performing time-lagged regression on the odor probabilities to calculate

This step aims to correlate the activity from adjacent bins to yield βs which signify the likelihood of a specific odor's replay followed by another odor's replay Δt milliseconds later. Specifically, this step utilizes the "sequenceness" metric designed by the authors of the MEG paper (90-91). The sequenceness metric involves performing time-lagged regressions which can be expressed as follows:

$$\hat{Y}_i = \sum_{j=1}^{5} X_j(\Delta t)\beta_{ji}(\Delta t)$$

Here, $\hat{Y}i$ is the odor probability for an odor *i* at time *t* (i.e., odor probability values from applying the odor classifier at time *t* for odor *i*). $Xj(\Delta t)$ is the predictor matrix and represents odor probability of specific odor at time $t\text{-}\Delta t$. The probabilities of all odors at the previous time point ($t\text{-}\Delta t$) are used to predict probability of a odor i at time t by taking a linear combination as shown in the formula above. Thus, by regressing $Xj(\Delta t)$ on every $\hat{Y}i$, (five $\hat{Y}i$, one for each odor), we can calculate $\beta(\Delta t)$, a *5x5* regression coefficient matrix expressing the degree to which the reactivation of each odor can be predicted by the reactivation of every other odor at time lag Δt. The time-lagged regressions are performed on the probability distributions obtained from adjacent 25 ms bins (i.e., Δt = 25ms) meaning that the data used for each regression does not overlap. The βs will be used in the following steps to identify replay moments and determine distribution of forward and reverse moments across the different intervals.

Step 4: Determining the forward and reverse replay of odor pairs

Here, for each β, we first built a distribution of its values obtained by computing time-lagged regressions across all intervals. Next, we focused the analysis on specific βs out of the 25 βs obtained from every time-lagged regression. To identify forward replay moments, we focused

on βAB, βBC, βCD, and βDE (highlighted in red in step 4 of Fig 3.1), whereas for the reverse replay we focus on βBA, βCB, βDC, and βED (highlighted in yellow in step 4 of Fig 3.1). Here, each β represents the replay of consecutive odors in either forward or reverse order.

Step 5: Determining the forward and reverse moments of involving 2 + consecutive odors

In this step, we computed consecutive βs to determine replay involving sequences of more than two odors. To do so, we focused the analysis on the same βs described in step 4. Specifically, we aggregated the consecutive forward and reverse βs from adjacent bins to quantify replay of consecutive odor sequences represented by the βs used in the sum. Three different sum types were considered separately for forward and reverse replays (for forward replay: sum of β A-E, β B-E, and β C-E, and for reverse replay: sum of β E-A, β D-A, and β C-A). β included in each sum type reflects the replay of corresponding odors in that order (e.g., consecutive βA-E quantifies the replay of odors A-E, by aggregating βAB, β BC, β CD, and β DE from adjacent non-overlapping 25ms bins).

Step 6 and 7: Identifying replay moments

To identify replay moments involving sequences of consecutive odors, we used the individual forward and reverse βs from step 4, and the consecutive βs from step 5. Specifically, we assessed the statistical significance of each β by applying a significance threshold of 3 standard deviations (i.e., β is significant when it exceeds its own mean by 3 standard deviations, where the mean is calculated based on that βs values across all intervals). Next, periods during which these β values are significant were marked as periods when the replay of the odor sequences were significant. We referred to these periods as replay moments and evaluated our

specific sequence replay predictions by examining the distribution of significant βs across various interval types.

3.2.3. NORMALIZING COUNTS OF SIGNIFICANT INDIVIDUAL AND CONSECUTIVE βs

The objective of this step is to make a fair comparison of the counts of significant individual βs and the consecutive βs across different interval types. Since the duration and trial counts differ among the intervals, we normalized the raw counts of significant β occurrences to the time bins within each interval type. Specifically, we computed the normalized count by using (i) the raw count value for individual βs or consecutive βs, (ii) the total number of 25ms bins in each interval type (i.e., the total number of time-lagged regression performed within each interval type), and (iii) the total number of 25ms bins for the shortest interval across all the types. We used the equation below to compute the normalized counts:

$$\text{Normalized count of } \beta \text{ in interval X} = \frac{\text{Count of } \beta}{\text{Bins in interval X}} \times \text{Bins in the shortest interval}$$

Where, the 'Count of β' is raw count of the number of times individual or consecutive β is significant (steps 4 and 5), interval *X* is one of the six interval types, and the multiplication term ('Bins in the shortest interval') is a constant for the different normalized counts.

3.4. RESULTS

Here, I describe our results on determining essential parameters of the framework obtained from analyzing CA1 activity. The next chapter (chapter 4) describes our neuroscience results from applying this framework to test specific replay predictions on the content and direction of replay moments.

3.4.1. DETERMINING THE OPTIMAL WINDOW FOR MODEL TRAINING

First, to develop the multinomial classifier, we determined the optimal time window during stimulus presentation that provides the highest prediction accuracy of the stimulus identity based on the ensemble activity within that window. We achieved this by building classifiers using various windows during the stimulus presentation (tested using 25 ms sliding windows across the odor presentation period). Our findings from 10-fold cross validation revealed that the 300-500 ms period following nose poke-in across all animals produced the most accurate results (Fig 3.2 A, B).

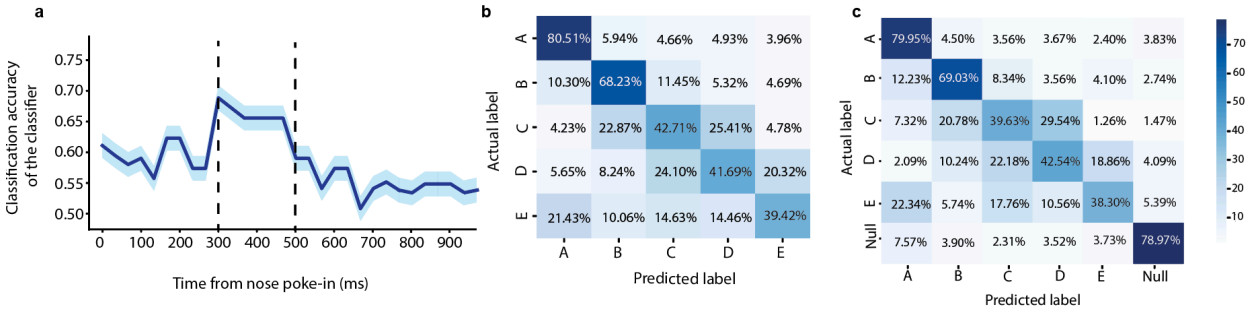

Fig 3.2. | Performance of the multinomial classifier. (a) Average classification accuracy across animals using ensemble activity from different windows during odor presentation. Plot shows 300 – 500 ms period from nose-poke in as the optimal time window for model training. **(b)** Confusion matrix showing average classification accuracy. Accuracy values obtained using 10-fold cross-validation when the model was trained on ensemble activity in the 300-500ms interval following nose-poke in. (c) Performance of the multinomial classifier on including the null state. Adding a null state to the classifier, does not impact classifier accuracy (obtain using 10-fold cross-validation on 300-500 ms after nose-poke in).

3.4.2. EVALUATING THE EFFECTS OF ADDING A NULL STATE TO CONTROL FOR MULTI-COLLINEARITY

Next, we introduced a null state to the classifier (as the 6th state, in addition to the 5 states representing odors A-E), to prevent multi-collinearity issue while performing time-lagged

regressions on the odor probabilities. Multi-collinearity occurs when covariates in a regression model are highly correlated, causing issues in accurately estimating the model's parameters. In our context, without the null state, the sum of odor probabilities would aggregate to 1, allowing the value of any one odor probability to be inferred as 1 minus the sum of the others, thus leading to multi-collinearity. We defined the null state as the ensemble activity during periods not overlapping with the 5 stimuli presentations (odors A-E that are the other 5 states of the classifier) and intervals where the classifier is applied. Specifically, we selected a 200ms window when the animal is running to receive a reward at the end of the maze after sequence completion, as this period is distinct from the other 5 states and the intervals between odor presentations. Importantly, we observed that including the null state maintained the classifier's performance, as indicated by similar results in Fig 3.2 B, C.

3.4.3. IDENTIFYING THE OPTIMAL TIME LAG BETWEEN BINS (ΔT)

Next, we focused on identifying the most effective Δt, an essential parameter of our framework, representing the time gap between bins within replay moments. To determine the optimal Δt, we utilized the approach from the MEG paper, which involves computing a "sequenceness measure." This measure quantifies the strength of the predicted replay content and contrasts it with replay containing random content (i.e., what we would expect by chance).

The sequenceness measure is calculated by taking a dot product of the individual βs that indicate replay of consecutive odors (our predicted replay - βAB, βBC, βCD, βDE) from each time-lagged regression and comparing this with chance levels. The chance levels are derived by permuting the labels of the 25 βs from each time-lagged regression and then computing the dot product of the same 4 individual βs but with permuted labels. This process essentially measures how much stronger the replay involving the odors of interest is compared to other odors for a specific Δt across all intervals. A higher sequenceness measure indicates stronger replay. We found that a Δt of approximately 25 ms yielded the highest sequenceness measure (Fig 3.3). We used this as a fixed parameter in the framework when applying it in chapter 4.

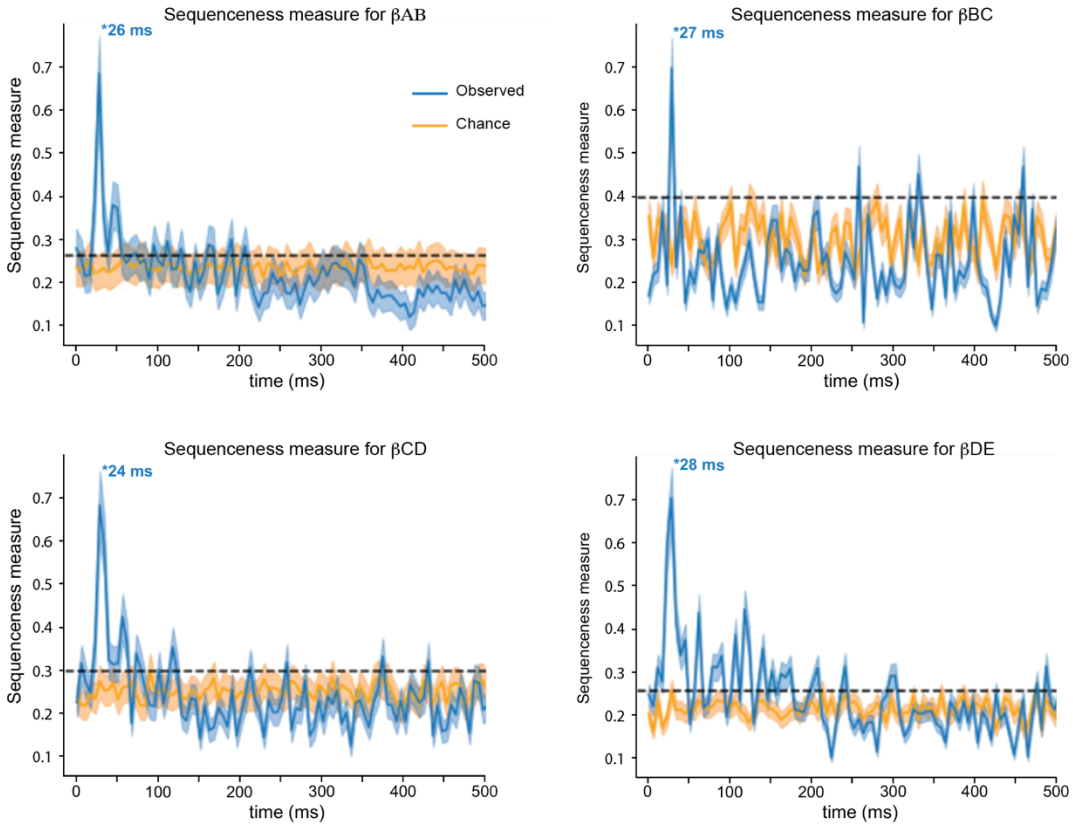

Fig 3.3. | Sequenceness measure using different Δt. Each plot shows the sequenceness measure using different Δt values on the four forward βs quantifying replay of consecutive odor pairs. Blue line shows the observed measure, and orange shows the measure obtained by chance. The shaded region for observed and chance measures show the 95% confidence interval. Black dotted line

marks the highest chance measure across all the Δt within a plot. All the plots show that the sequenceness measure is the highest when Δt is around 25ms.

3.4. DISCUSSION

In this chapter we built a strong statistical framework that addresses the limitations of the previous models and determines sequence replay of discontiguous states during resting periods. Our neuroscience findings using this framework are in line with prior results (discussed in chapter 4), supporting the validity of our framework. Briefly, the objective of this framework is two-folds: (i) identify replay moments involving sequence replay of non-spatial information during intervals between odor presentations, and (ii) determine whether the direction and content of sequence replay matches our predictions. To accomplish this, we developed a statistical framework that incorporated the "sequenceness metric" previously used in a human MEG study (90-91) to evaluate sequence coding. In its original form, this metric can identify replay moments for pairs of events but cannot quantify the replay of multiple events or their exact temporal sequence. In our framework, we expanded this metric to detect replay moments involving sequences of two or more odors and to determine the precise order in which they are replayed. Given the complexity of our task design and the difference in data modalities (MEG vs. electrophysiology), we adapted this metric to fit our data, task requirements, and the need to test specific sequence replay predictions. This adaptation involved creating a model to predict odor identity based on ensemble activity and verifying whether the distribution of replay moments across intervals of varying lengths matched our predictions.

Recent advances have shown that not all significant spatial replay occurs within detected SWRs, suggesting that rapid, time-compressed replay might not always coincide with SWRs (39,

106, 145-146). Despite this, most existing methods focus on analyzing ensemble activity during SWRs to study replay events (39, 41 105, 145-146). A further complication is that these methods assume replay events not only coincide with SWRs but also start at the same time. However, the detection of SWRs depends on specific thresholds that vary between studies, making the boundaries of detected SWRs sensitive to these thresholds and potentially imprecise (142). In this framework, we detect replay moments during resting periods independent of SWRs. This enables us to perform a post-hoc analysis to determine how many detected replay moments overlap with SWRs or other potential moments of interest.

This statistical framework allowed us to test our specific replay hypothesis and provided us with insights into hippocampal replay in a nonspatial sequence memory task. The neuroscience results are shown in the next chapter (chapter 4). Here, I describe how we can expand this approach and address its potential limitations. Using this method for tasks that involve novel odor sequences (like Novel session 1 and 2 involving presentation of a novel sequence VWXYZ with the same task rules as in our current task) presents challenges because training a classifier to differentiate odors based on ensemble activity is difficult while animals are actively developing representations of these new sequences. To analyze data from novel odor sequences, this framework will require modifications, possibly including the use of template matching or similar techniques to identify evolving patterns in the ensemble activity associated with stimulus identity. Research has demonstrated that hippocampal replay can happen at varying speeds. However, our existing framework only accommodates a fixed replay speed and duration, determined by the fixed Δt value. For example, with a Δt of 25 ms, a replay moment involving two odors lasts 50 ms, one replaying three odors lasts 75 ms, and so forth. Further research is required to implement Δt as a learnable parameter to accommodate these varying

replay speeds. We include a null state to prevent the sum of odor probabilities used in time-lagged regression from aggregating to one to address collinearity issues. In the future, we will explore other ways to address this potential problem.

CHAPTER 4: DETERMINE IF HIPPOCAMPAL REPLAY REPRESENTS SEQUENCES OF DISCRETE NONSPATIAL STATES DURING OFFLINE PERIODS

4.1. RATIONALE

The ability to rapidly replay sequences of experienced or expected events during offline periods is thought to be critical to a variety of cognitive functions, ranging from the formation and consolidation of memories to decision-making and planning (103, 115-118, 132). Experimental evidence supporting this theoretical framework comes primarily from spatial navigation studies in rodents, which show that hippocampal representations of visited locations can be sequentially replayed during sleep or during brief moments of rest during task performance (41, 105-106, 132-133). More precisely, these studies have shown that the sequence of hippocampal 'place cells' activated during the traversal of a path can be rapidly replayed in the original or reverse order, known as forward and reverse replay, respectively. Forward replay predominantly occurs before path traversal and contains representations of trajectories leading to a goal, suggesting a role in the planning and evaluation of upcoming behavior (38, 107-108, 121-122, 137). Conversely, reverse replay tends to occur after path traversal and is associated with reward delivery, suggesting a role in connecting recent behaviors with their outcomes to facilitate the formation and consolidation of memories (38, 41, 60, 111, 121-122, 144).

Considerable research has shown that the fundamental role of the hippocampus in memory is conserved across stimulus modalities and across species (3, 15, 28, 48-49, 68). In recent years, prominent theoretical and computational models have integrated key evidence from the place cell literature with the behavioral and functional literature across species to propose

unifying principles of hippocampal organization and representation that are content-agnostic and thus could support this range of function. A central prediction of this emerging conceptual framework is that the same principles that underly replay of continuous trajectories (states that are adjacent in space and time) could extend beyond the spatial domain and give rise to replay of complex non-spatial sequential relationships extracted by the hippocampal network across daily life experiences (156-160). However, to date, there is no direct evidence that hippocampal ensembles can replay sequential relationships among discrete non-spatial events.

Here we address this critical gap through a challenging combination of behavioral, electrophysiological, and statistical approaches. More specifically, we recorded hippocampal ensemble activity as rats performed a complex non-spatial sequence memory task, which tested their memory for sequential relationships among discrete events. Importantly, the task also included intervals of a few seconds between stimuli, offline periods during which animals briefly rested and consumed a reward, to parallel conditions known to favor sequence replay dynamics in spatial paradigms. We then implemented a rigorous statistical framework to capture replay for sequences of discrete (non-continuous) states (described in chapter 3) and tested key predictions derived from the spatial and computational literature about the direction and content of replay across intervals.

We provide the first direct evidence of replay for learned sequential relationships among discrete non-spatial events, with a pattern of forward and reverse replay similar to that observed in familiar spatial environments. Forward replay was primarily observed during the rest intervals separating each event of the sequence and represented upcoming parts of the sequences. In contrast, reverse replay was less frequent and predominantly clustered in the intervals at the end of the sequence. These findings strongly suggest that hippocampal sequence replay can extend to

other modalities and capture more complex cognitive demands, providing compelling evidence for computational and theoretical models proposing a fundamental and content-agnostic role for hippocampal replay in learning, consolidating, and retrieving multi-step associations to guide goal-directed behavior.

4.2. APPROACH

4.2.1. DATA

This chapter utilized the same dataset as in chapter 2 but here, I focused on analyzing different epochs. While chapter 2 analyzed ensemble spiking during stimuli and entire sequenceness presentation (spanning across different stimuli presentations and intervals separating them), this chapter analyzed the information contained particularly during intervals across the entire session. I focused on the intervals as they are analogous to the brief resting periods observed during behavior on spatial studies and during which replay events are shown to occur. Refer to chapter 3 (3.2.1) for more information on the interval numbers, duration etc.

4.2.2. SUMMARY OF APPROACH

To test our specific replay hypotheses, we used the statistical framework described in chapter 3. Briefly, this framework incorporates the sequenceness metric, previously developed to quantify replay of non-spatial events in an MEG study (90-91), and we expanded this metric to: (i) identify replay moments involving sequences of consecutive odors replayed in both forward and reverse direction (ii) investigate whether the distribution of these forward and reverse replay moments across intervals aligns with our predicted patterns (Fig 4.1).

To develop our hypothesis, we drew from predictions in the spatial and computational literature about the nature and direction of replay across intervals. We aimed to determine if the replay content mirrors the task structure by depicting task critical information of sequences of discontiguous odor presentations leading to goal, excluding the time between these events. We predicted that both forward and reverse replay moments will occur during intervals. Specifically, we proposed that forward replay moments will be more prevalent during intervals within sequence presentation (before odor E) and will represent upcoming odor sequences (starting from the current position in the sequence or remote replays, starting from other odors in the sequence). On the other hand, we predicted that reverse replay moments will be more prevalent towards the end of the sequence presentation (after odor E) and will include consecutive odors from the sequence (beginning with odor E or will be remote, starting from other odors in the sequence). Refer to Fig 4.1 for an illustration of our predicted working model, and to 3.1 for an overview of our framework.

Note that we applied our statistical framework to all time bins contained in intervals, not just around SWRs. Using SWRs to align the decoding of repay events is a common approach, as it is a convenient way to narrow down the number of bins examined, but doing so is less important with our approach because we are building the distribution of all possible values. Since it was previously documented that sequence replay is common outside of SWR events (137, 145-146), our primary focus is on capturing all potential replays. Comparisons between replays occurring during and outside of SWRs can still be performed as secondary analyses.

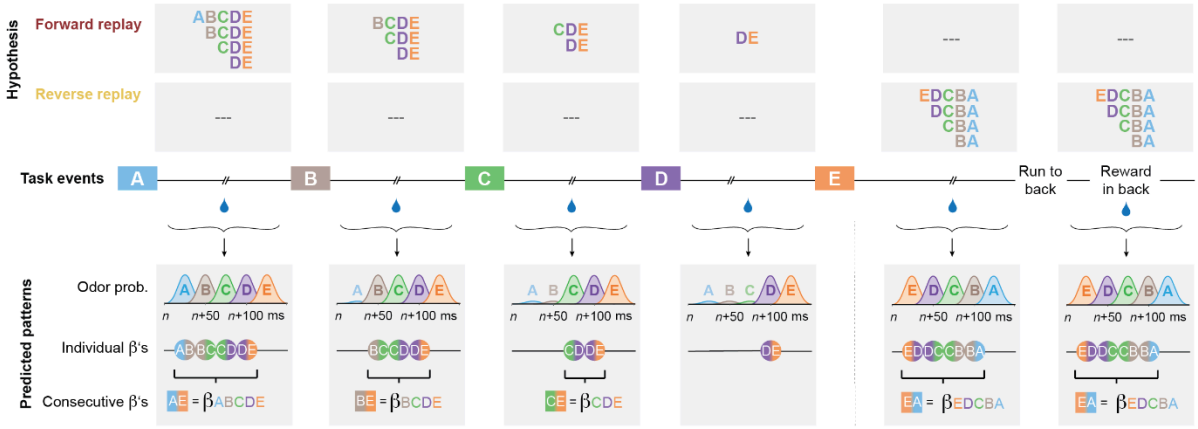

Fig. 4.1. | Working model of predicted distribution of replay moments across intervals. Predicted distribution of significant forward and reverse replay moments across intervals. *Top*, Forward replay moments are expected to cluster during intervals of the sequence and reflect upcoming parts of the sequence. Since animals are already well-trained on this sequence, reverse replay moments are expected to be less frequent and to cluster at the end of the sequence. Note that both forward and reverse replay can start locally (e.g., with adjacent odor) or remotely. *Bottom*, Depiction of an example local replay for each interval, including the idealized sequential pattern of odor probabilities and the corresponding significant individual and consecutive βs capturing them.

4.2.4. SWR IDENTIFICATION

Automated SWR detection was performed by adapting a published approach. A SWR event was identified as the co-occurrence of a sharp-wave event and of a ripple event detected on two separate tetrodes (electrode closest to CA1 stratum radiatum for sharp wave events and electrode closest to the center of CA1 pyramidal layer for ripple events). For both sharp wave and ripple events, the LFP was first filtered (sharp wave > 4 Hz; ripple: 150-250 Hz), and instantaneous power was calculated as the real component of the Hilbert transformed trace. Putative events were identified as periods where power exceeded three standard deviations above the mean. Periods that occurred within 15 ms of each other were considered part of a common event. SWRs were then identified as periods of temporal overlap between putative sharp wave and ripple events, which

were verified through visual inspection. Temporal boundaries for SWRs were determined as the earliest and latest timepoints of either the sharp wave or ripple events identified.

4.2.5. LFP ANALYSIS

The raw data underwent preprocessing via a Butterworth notch filter to eliminate 60 Hz line noise. For spectral analysis, we employed a continuous wavelet transform using the SciPy signal processing toolbox in Python. This produced analytical wavelets across frequencies spanning 3-300 Hz. Subsequently, we extracted instantaneous power within specified frequency ranges during the three moment types (replay, SWRs, and control which are randomly identified and do not coincide with replay or SWRs) and represented this through spectrograms. Power shown in the spectrograms is presented as z-score values relative to the mean and standard deviation of power for a given frequency, calculated from the entire session's recordings using the same electrode.

4.2.6. DETERMINE ODOR SELECTIVE NEURONS AND VISUALIZING THEIR ACTIVITY DURING REPLAY MOMENTS

To determine odor-selective cells (i.e., neurons selective of specific odor type(s)), the LASSO logistic regression model from Step 2 of Fig 3.1 was built for each neuron separately. Specifically, for each neuron, using 10-fold cross-validation with stratification, a model was trained and tested on 200ms spiking activity during odor presentations (300-500ms after port entry), separately. The performance of each model on the test data determined the neuron's selectivity for single and/or multiple odors. The accuracy of the model was evaluated using the d-prime value, which served as a measure of the model's performance. If the d-prime value surpassed a threshold of 1 for specific odor(s), the neuron was identified as selective for that odor(s). This

approach allowed for the identification of neurons that exhibited selectivity for either a single odor or a combination of odors.

To visualize the activity of odor selective neurons during replay moments, we used PSTHs. We averaged the activity of each odor selective neuron during all moments of a specific replay type (e.g., all replay moments of A-E, and separately for all replay moments of B-E). Next, we normalized the mean activity of each neuron by comparing its mean activity during all other replay types. Specifically, we divided the mean activity of the neuron with its peak activity across all other replay type.

4.3. RESULTS

Here we leveraged our unique experimental design to determine whether the phenomenon of sequence replay often observed during rest periods between bouts of spatial exploration extends to other domains. A key feature of our design are the intervals between odors (Fig 2.1), which offer a strong parallel to the rest or offline periods of spatial paradigms. In fact, during our intervals, animals receive a small reward, and the local field potential activity is characterized by a reduction in theta power (relative to odor sampling and running; 60, 161) and the presence of SWRs (see Fig 4.9.). We focused our analyses on the ensemble activity during those intervals and specifically examined whether the neural representations of the odors were sequentially reactivated during these offline periods.

4.3.1. CA1 ENSEMBLES REPLAY THE SEQUENCE OF EXPECTED UPCOMING EVENTS BEFORE EACH EVENT IN THE SEQUENCE.

Evidence from the place cell literature has shown that hippocampal ensembles often replay the series of locations leading to a goal (38, 105, 121, 134, 137), suggesting a role for forward replay in planning and evaluating potential upcoming trajectories (105-106, 108, 122). If this phenomenon reflects a fundamental function of the hippocampus, then it should extend to other stimulus modalities and, when challenged with more complex task demands, should abstract the corresponding steps and goals critical to performance. Here we directly test this by determining whether forward replay in CA1 ensembles can capture task-critical abstracted sequential relationships among discrete nonspatial states widely separated in time.

To achieve this, we took the significant consecutive β representing forward sequence replay moments (e.g., βABCDE), identified using the unbiased approach described in the previous section, and tabulated their counts across the "rest" intervals separating each item of the sequence (Fig 4.2). For each β, we normalized the counts across interval type (i.e., across rows in Fig 4.2 C) to account for variability in the duration and number of intervals. Specifically, the raw counts were divided by the number of possible bins for a given interval and normalized to the interval with the fewest bins (interval between D and E). We tested the hypothesis that forward replay reflects the animal's expectations for upcoming parts of the sequence (or steps toward the "goal" that represents the end of the sequence). Note that such forward replay may start locally (with the closest odor, e.g., replay BCDE during intervals adjacent to B) or remotely from a future sequence position (e.g., CDE when adjacent to B), but *not* from a remote past sequence position (e.g., BCDE when adjacent to D) nor after completion of the sequence (after E). This leads to testable predictions for the counts of each forward replay type across interval types with

the boundary condition being whether the most recently presented odor exceeds the replay's start item (darker grey boxes in Fig 4.2 C). For each forward replay type, counts were hypothesized to be significantly higher for intervals before that boundary (e.g., CDE before D) than after (e.g., CDE after D). Note that we do not have a comparable "rest" interval before odor A as animals immediately nose poked upon arriving at the odor port.

Consistent with the hypothesis, βABCDE moments were significantly more prevalent in the first interval (interval after odor A), βBCDE moments in the first two intervals (before and after B), βCDE in the first three intervals, and βDE in the first four intervals. The same pattern of results was observed when examining the distribution of individual forward βs (see Fig 4.3). These findings are consistent with the literature on spatial replay and extend the phenomenon to complex sequential relationships across discrete events, suggesting that forward replay can support the evaluation of potential sequences of states toward goals that are more abstract or associative in nature.

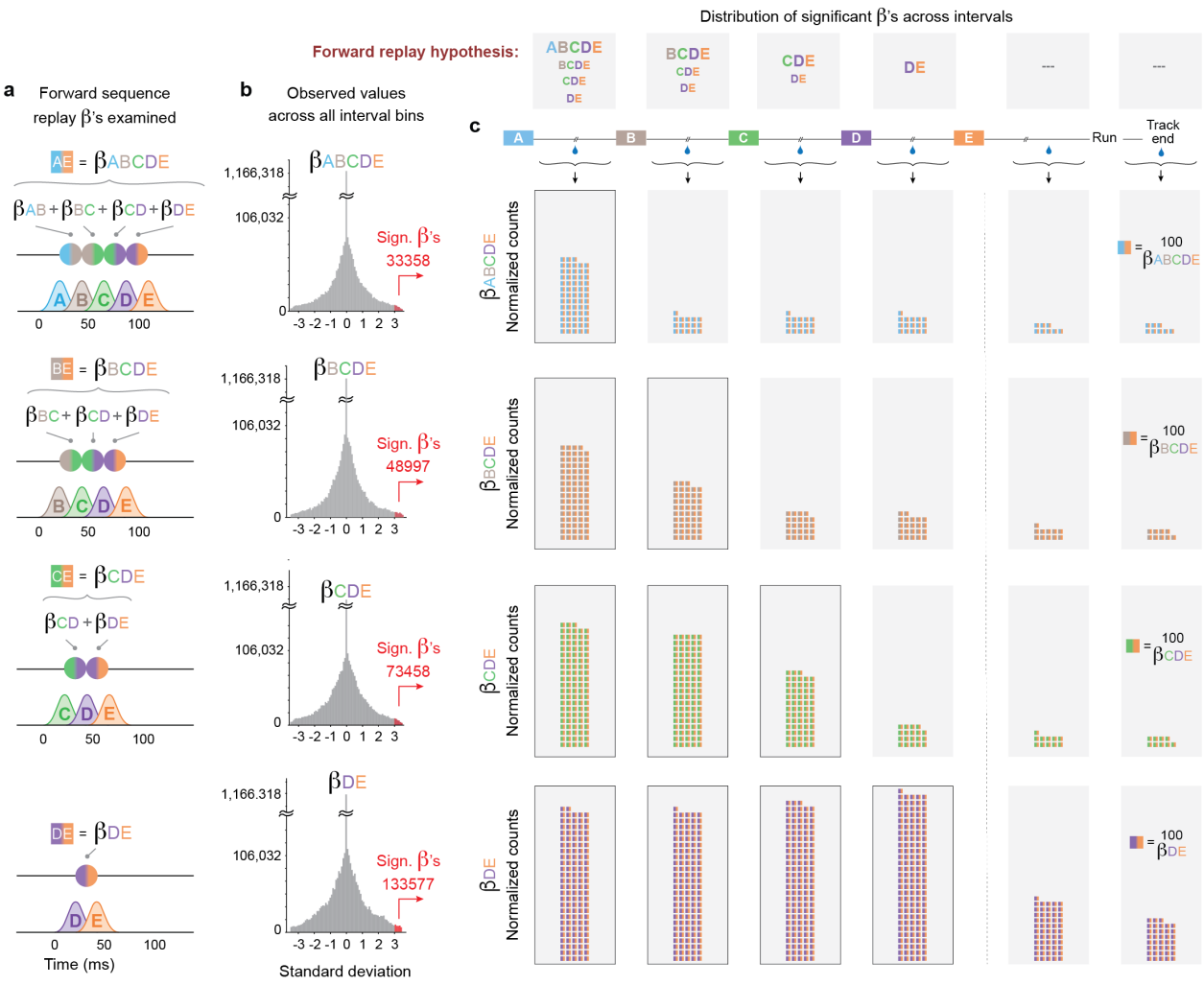

Fig. 4.2. | Forward sequence replay of discrete nonspatial events occurs during intervals before each event in the sequence. (a) Schematic of the four types of βs used to capture moments of forward sequence replay in the ensemble activity (βABCDE, βBCDE, βCDE, βDE). **(b)** Frequency distribution of all regression values observed for each β type across all interval time bins and animals. Significant βs were identified as moments in which the regression value was 3 standard deviations above the mean (computed separately for each animal). **(c)** The counts of significant βs observed for each replay type matched the predicted pattern across intervals. Each gray box displays the counts of significant βs for the corresponding replay type and interval type (aggregated across trials and animals), normalized within each row to the interval type with the fewest time bins (i.e., the interval between D and E). Each square represents 100 normalized counts. Boxes in which counts were predicted to be higher are indicated by a black outline. Replays starting with a non-adjacent event representation were considered remote replays (βCDE in first interval, and βDE in first two intervals), and others local replays.

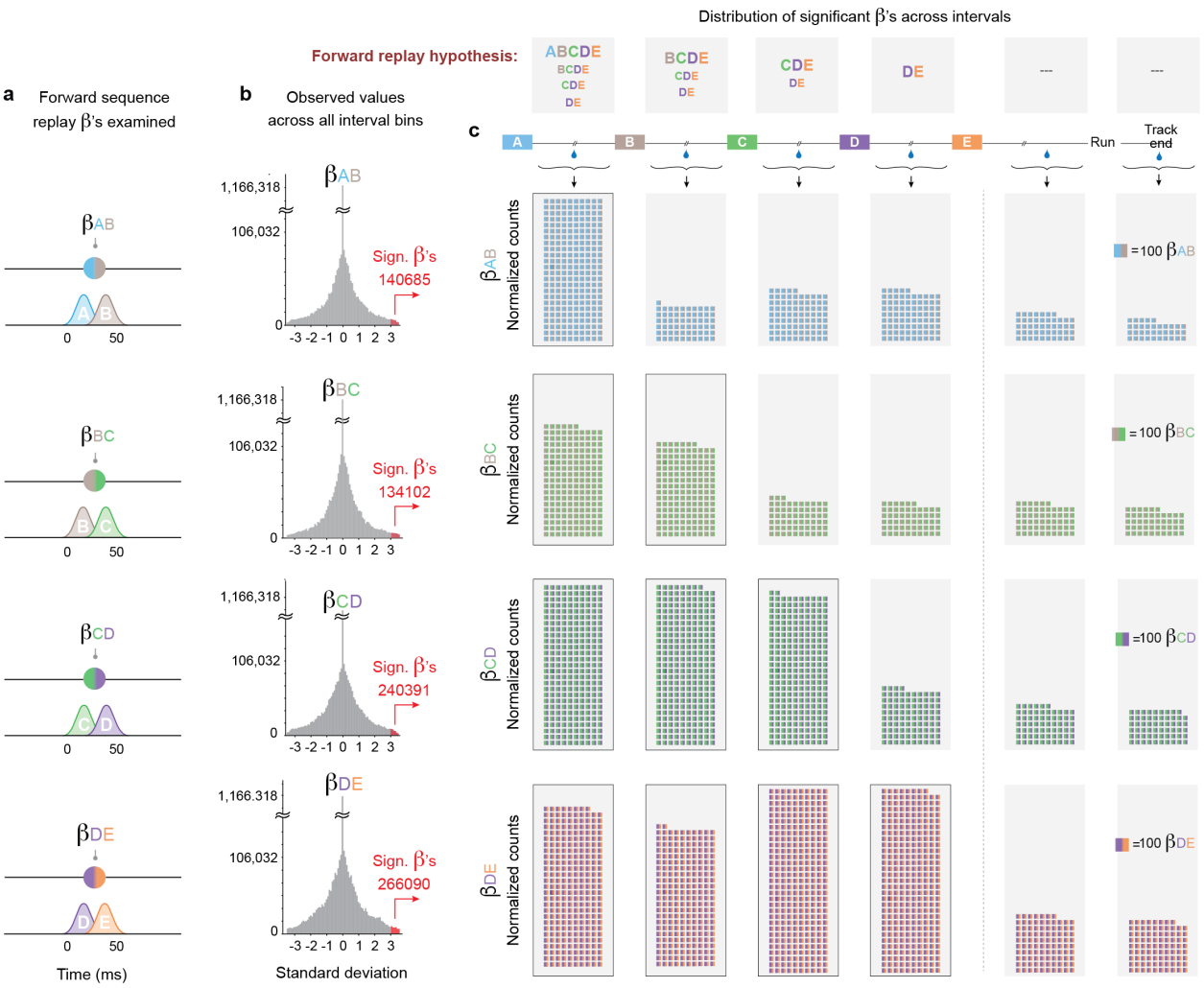

Fig. 4.3. | Forward sequence replay quantified by the individual forward βs display similar patterns. (a) Schematic of the four types of individual forward βs used to capture moments of forward sequence replay of consecutive odor pairs (βAB, βBC, βCD, βDE). **(b)** Frequency distribution of all regression values observed for each β type across all interval time bins and animals. Significant βs were identified as moments in which the regression value was 3 standard deviations above the mean (computed separately for each animal). **(c)** Similar to Fig 4.2, the counts of significant βs observed for each replay type matched the predicted pattern across. As in Fig 4.2, each gray box displays the normalized counts of significant βs across replay and interval type (aggregated across trials and animals, normalized within rows intervals between D and E), and each square representing 100 normalized counts. Boxes in which counts were predicted to be higher are indicated by a black outline. Replays starting with a non-adjacent event representation were considered remote replays (βCD in first interval, and βDE in first two intervals), and others local replays.

4.3.3. VISUALIZING THE ENSEMBLE ACTIVITY DURING SIGNIFICANT REPLAY MOMENTS.

While our main analyses focused on categorical data (counts of significant replay moments across intervals), we thought it would also be informative to visualize the information contained in the ensemble activity during each replay type. Although our replay results are based on decoding activity from entire ensembles, many informative neurons have complex coding patterns (e.g., selectivity for multiple odors) that are difficult to visualize. Therefore, as in our previous work (153), we found that the best way to visualize this was to highlight the activity of odor-selective neurons (neurons selective for a single odor). To do so, we identified odor-selective neurons by applying the classifier to each neuron individually (see 4.2.6). Subsequently, for each type of replay, we visualized the activity of the five different types of odor-selective neurons (neurons aggregated across subjects). The activity of each neuron was normalized to its peak activity using all replay events (see methods) to facilitate comparisons across plots.

The pattern of activity in odor-selective neurons matched the expected content of each replay type (Fig 4.4). More specifically, we observed sequential firing patterns which followed the order in which the decoded odor information was replayed. For instance, during βABCDE moments, neurons selective for odors A, B, C, D, or E were active in that order. During βBCDE moments, a similar pattern was observed with the exception that odor A neurons did not significantly increase their firing and so on. Importantly, such sequential activity patterns were not observed when data was permuted or during moments selected at random during the intervals (Fig 4.5). These visualization results validate that the information contained in the ensemble activity is consistent with the expected content of replay moments identified using β.

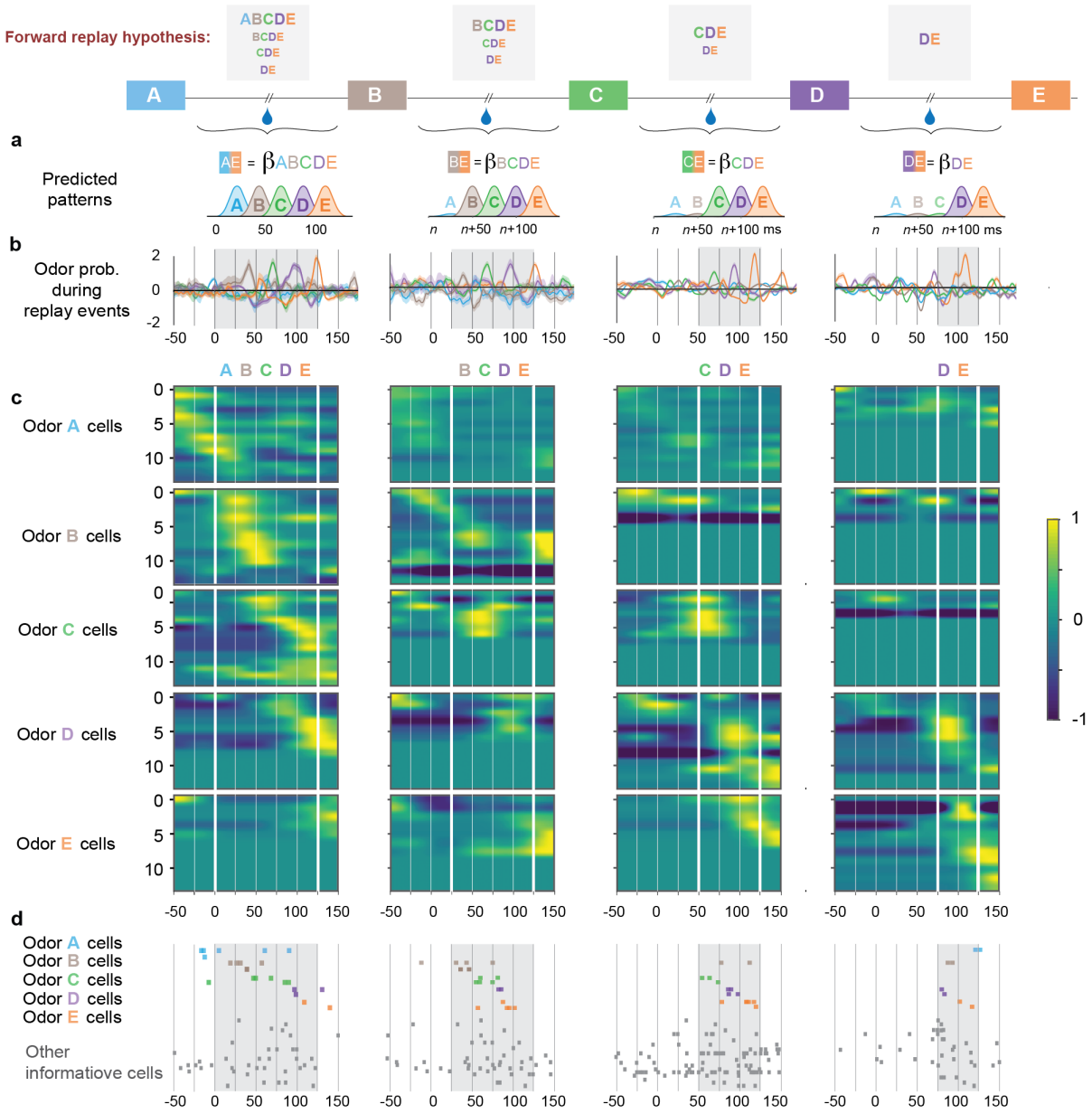

Fig. 4.4. | Visualization of forward sequence replay moments using the activity of odor-selective neurons. (a) Schematic of the four types of significant βs (βABCDE, βBCDE, βCDE, βDE) visualized across the four interval types. **(b)** Information represented in the ensemble activity during the corresponding significant βs moments. Odor probabilities are averaged across moments and across subjects (mean +/- SEM). **(c)** Corresponding peri-stimulus time histograms (PSTHs) showing the average single-cell activity for the subset of neurons selective to each odor (13, 12, 13, 14, and 13 neurons selective for odors A, B, C, D, and E, respectively; neurons aggregated across animals). For clarity, only neurons selective to a single odor are included, the activity of neuron is normalized across columns, and neurons are sorted by their time of peak firing in each PSTH. **(d)** Corresponding raster plots showing spikes from the same neuronal ensemble in a single instance of each type of replay (same sorting of neurons across raster's).

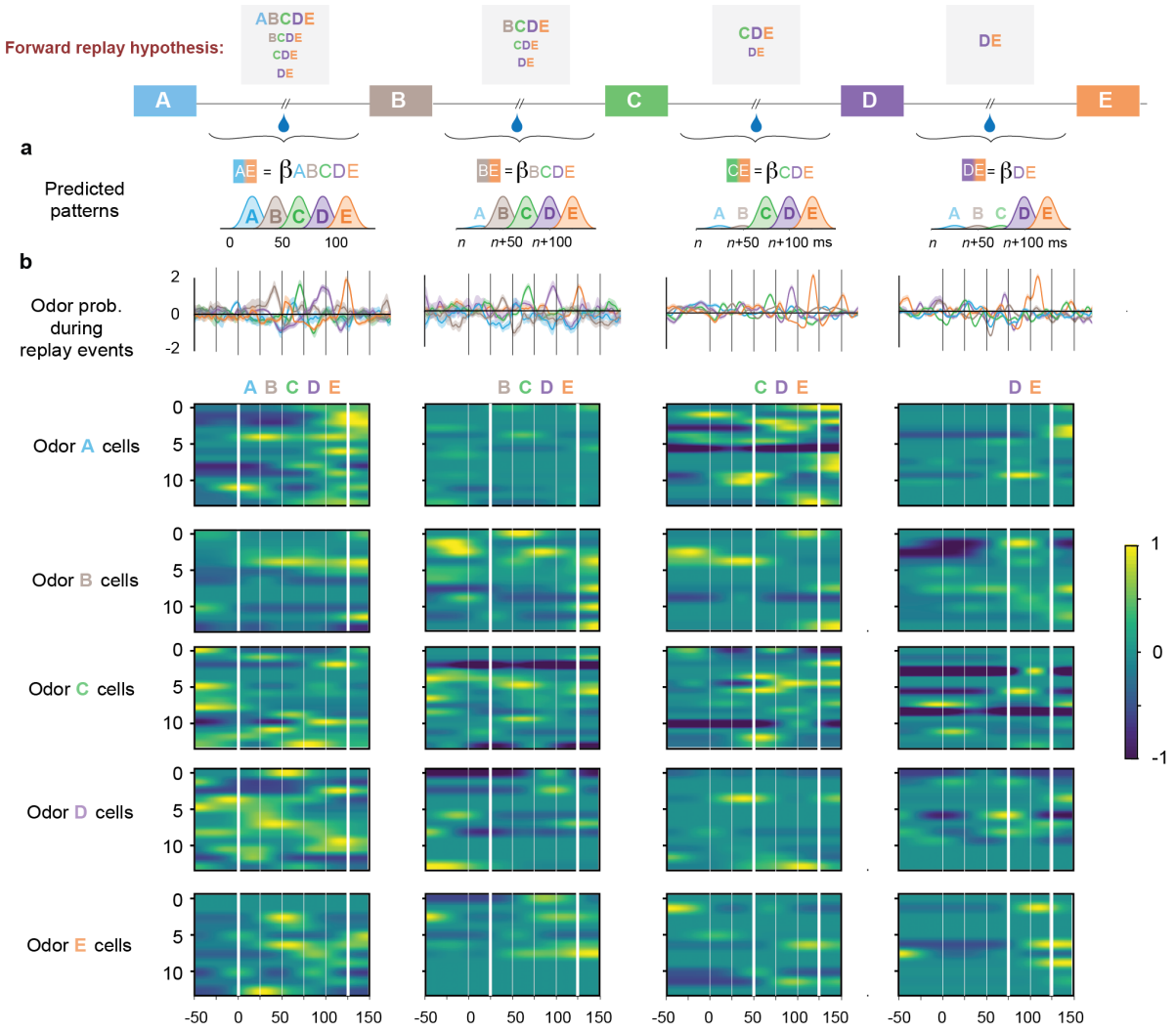

Fig. 4.5. | Visualization of odor-selective neurons during control moments. (a) Schematic of the four types of significant βs (βABCDE, βBCDE, βCDE, βDE) visualized across the four interval types. **(b)** Information represented in the ensemble activity during the corresponding significant βs moments. Odor probabilities are averaged across moments and across subjects (mean +/- SEM). **(c)** Peri-stimulus time histograms (PSTHs) showing the average single-cell activity for the subset of neurons selective to each odor (same neurons as in Fig 4.4) during control moments. Control moments are random moments picked from the intervals which do not overlap with replay moments and SWRs.

4.3.4. REVERSE REPLAY OF THE LEARNED SEQUENCE IS LESS FREQUENT AND PRIMARILY OCCURS AFTER THE END OF THE SEQUENCE.

Evidence from the place cell literature also indicates that hippocampal ensembles often replay recently travelled trajectories in the *reverse* direction upon reaching a goal location and that this form of coding is influenced by reward magnitude (105, 116, 144). Reverse replay has therefore been associated with a role in the formation and consolidation of goal-related memories (38, 41, 60, 111, 121-122). Here we directly tested whether the phenomenon of reverse replay extends to other modalities and complex task demands. In this specific case, there are two key aspects of the data to consider. First, although there is little new learning in the recorded session (the sequence is learned preoperatively), the presentation of out of sequence (OutSeq) items could interfere with the memory of the sequence. Thus, there is an incentive for the system to reverse replay the correct sequence upon completion. Second, upon successful completion of the sequence, a larger water reward was delivered at the other end of the track to encourage segmentation of the sequences. Although no odors are presented at that location, the larger reward may bias the system toward reverse replay dynamics. Consequently, unlike the pattern observed with forward replay, we hypothesized that reverse replay would be stronger at the end of the sequence (i.e., once the goal has been reached), that is both after odor E and after the larger reward is consumed at the other end of the track.

This hypothesis led to testable predictions for the counts of each reverse replay type across interval type, with the boundary condition being the last odor of the sequence (darker grey boxes in Fig 4.6 C). In other words, for each reverse replay type, counts were hypothesized to be significantly higher for intervals after odor E (e.g., EDCBA after E) than before (e.g., EDCBA before D). Like the approach used to quantify forward replay, we took the significant

consecutive βs representing reverse sequence replay moments (e.g., βEDCBA), tabulated their counts across the intervals of the sequence, and normalized the counts of each β across intervals (Fig. 4.6).

Consistent with the hypothesis, βEDCBA, βDCBA, βCBA, and βBA moments were significantly more prevalent in the two intervals after odor E presentation, though βEDCBA counts were also high before odor E. The same pattern of results was observed when examining the distribution of individual reverse βs (Fig. 4.7). These findings are consistent with the literature on spatial replay and extend the phenomenon to conditions in which learned representations must be maintained despite interfering events, suggesting that the role of reverse replay in not limited to the formation and consolidation of new learning.

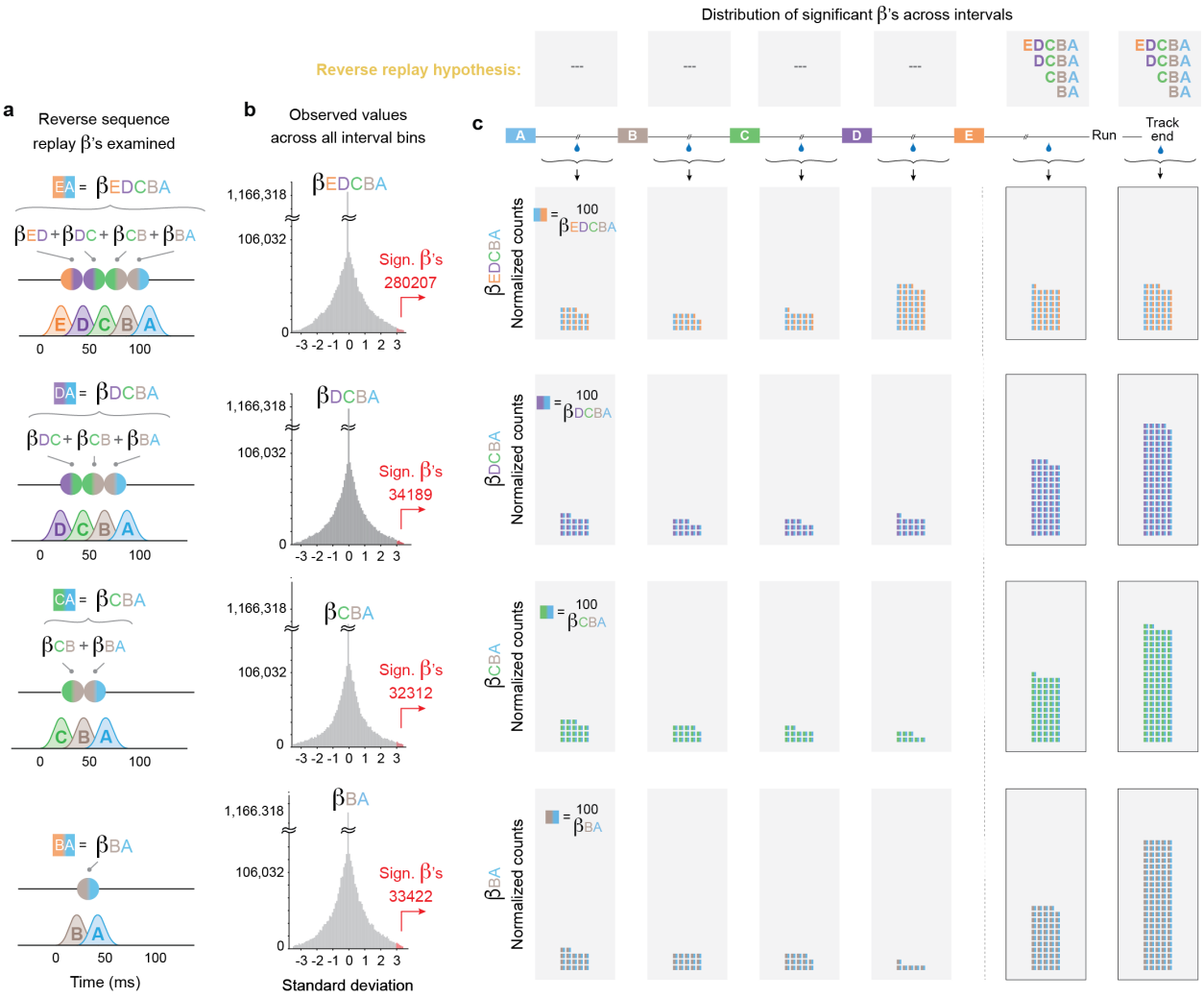

Fig. 4.6. | Reverse sequence replay predominantly occurs during intervals following the end of the sequence. (a) Schematic of the four types of βs used to capture moments of reverse sequence replay in the ensemble activity (βEDCBA, βDCBA, βCBA, βBA). **(b)** Frequency distribution of all regression values observed for each β type across all interval time bins and animals. Significant βs were identified as moments in which the regression value was 3 standard deviations above the mean (computed separately for each animal). **(c)** With one exception (βEDCBA counts in interval between D and E), the counts of significant βs observed for each replay type matched the predicted pattern across intervals. As in Figure 4.2, each gray box displays the normalized counts of significant βs across replay and interval type (aggregated across trials and animals, normalized within rows intervals between D and E), and each square representing 100 normalized counts. Boxes in which counts were predicted to be higher are indicated by a black outline. Replays starting with an adjacent event representation were considered local replays (βEDCBA in intervals before and after odor E) and others remote replay.

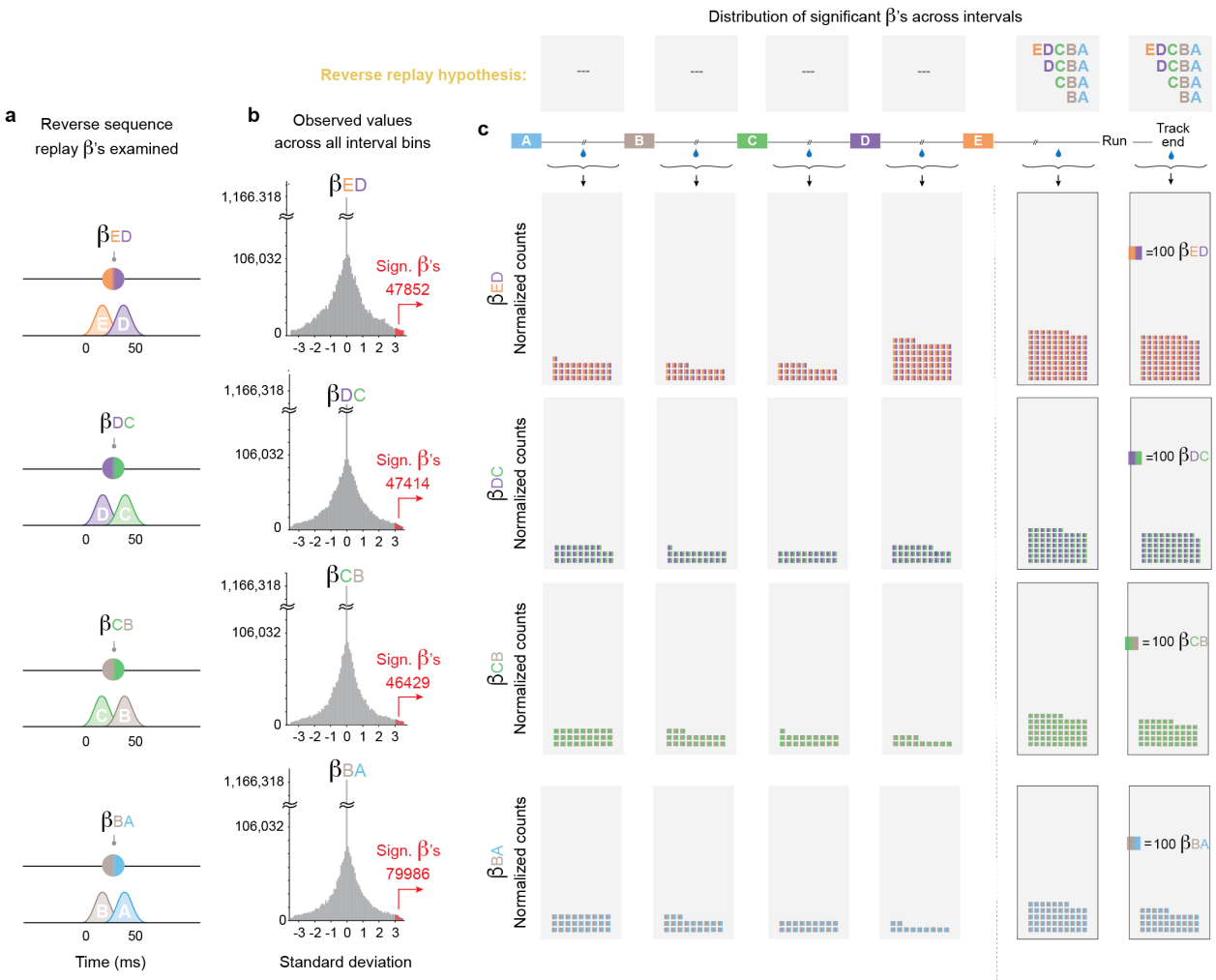

Fig. 4.7. | Reverse sequence replay quantified by the individual reverse β display similar patterns. (a) Schematic of the four types of individual reverse βs used to capture moments of reverse sequence replay of consecutive odor pairs (βED, βDC, βCB, βBA). **(b)** Frequency distribution of all regression values observed for each β type across all interval time bins and animals. Significant βs were identified as moments in which the regression value was 3 standard deviations above the mean (computed separately for each animal). **(c)** Similar to Fig 4.6, the counts of significant βs observed for each replay type matched the predicted pattern across intervals (with one exception of βED counts in interval between D and E. As in Fig 4.2, each gray box displays the normalized counts of significant βs across replay and interval type (aggregated across trials and animals, normalized within rows intervals between D and E), and each square representing 100 normalized counts. Boxes in which counts were predicted to be higher are indicated by a black outline. Replays starting with an adjacent event representation were considered local replays (βED in intervals before and after odor E) and others remote replay.

4.3.5. THE DISTRIBUTION OF REPLAY MOMENTS WITHIN INTERVALS PARTIALLY OVERLAPS WITH THAT OF SWRs AND IS INFLUENCED BY REPLAY DIRECTION AND START ITEM.

Prior research on sequence replay has primarily focused on analyzing ensemble activity during SWRs. While this approach is useful in limiting data analysis to potentially informative periods, there is no one-to-one mapping between the two. In fact, recent studies have shown that not all SWRs events exhibit replay, with the proportion of SWRs with replay ranging from 5% to 70% (109), and that replay frequently occurs outside of SWRs (137, 145-146). Therefore, to capture all replay moments, we analyzed the activity from all interval time bins rather than only those coinciding with SWR events.

We found that, on average, replay moments and SWRs exhibited similar distributions within intervals, with a peak near the middle of that period (Fig 4.8 B). However, when directly examining the overlap of individual SWRs and replay moments, we observed that 30% of SWRs coincided with replay moments (Fig 4.8 A). As mentioned above, this proportion is consistent with those reported in previous studies (105-106, 109, 137, 143, 162-164).

We then examined LFP power during replay moments using spectrograms (Fig 4.9). As expected, replay moments coinciding with SWRs showed high power in the 150-250 Hz band and lower power in other bands. For replay moments not coinciding with SWRs, we observed no distinctive increase in power across frequency bands. Similarly, no distinctive increase in power across bands was observed on control moments, which were randomly sampled from intervals but did not overlap with either SWRs or replay moments. These results are consistent with prior evidence that replay occurs during periods of irregular activity in the LFP observed during offline periods (137).

Interestingly, we discovered that the direction and starting item of replays influence their distribution within the intervals. First, we found that reverse replay was predominantly distributed early during intervals (Fig 4.8 C). This is not surprising given that the reward was delivered around 500 ms into the interval and that reverse replay shows a strong association with reward consumption. In contrast, we found the distribution of forward replay to be bimodal, with the two peaks reflecting different start items for the replay (Fig 4.8 D). Replays starting with the previous item occurred earlier during intervals (i.e., closer to the previous odor than the next), whereas replays starting with the next item occurred later during intervals (i.e., closer to the next odor). These findings provide important new information about the relationship between the content of replay and its timing in relation to task events.

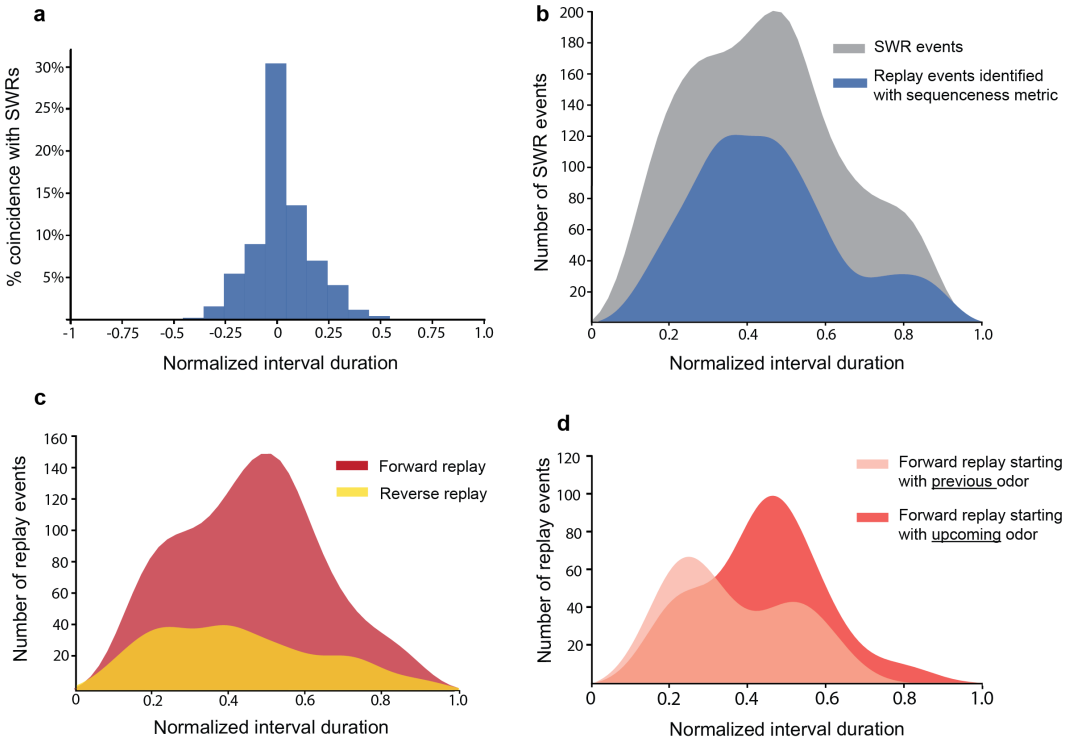

Fig. 4.8. | Distribution of replay moments and SWR events within intervals. (a) Percent coincidence between replay moments and SWRs. Since the duration of the intervals vary, we normalize the duration to its length, to make fair comparison of coincidence across intervals. 0 indicates start of the interval (poke-out from the previous odor), and 1 indicates end of the interval

(poke-in for the upcoming odors) **(b)** SWRs and replay moments are similarly distributed during the intervals, where both cluster in the middle of the interval. **(c)** Distribution of forward and reverse replay moments during intervals. Forward replay moments are more in number than reverse replay, which matches our predicted patterns. **(d)** Distribution of forward replay moments with different start content. Forward replay moments that start with the previous odor in the sequence (e.g., replay BCDE during interval after B) tend to cluster earlier than those that start with the upcoming odor (e.g., replay CDE during interval after B).

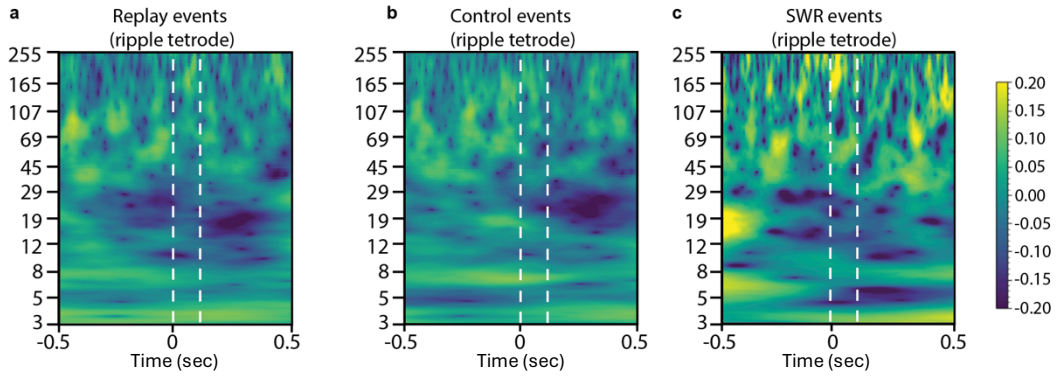

Fig. 4.9. | LFP power during replay moments, control moments and SWR events. (a) Spectrograms displaying the average power in the 3-255 Hz range for replay moments (βABCDE and βEDCBA), control moments and SWRs, each of 125 ms in duration. Control moments were randomly sampled from the intervals but did not overlap with the replay moments or SWR events. White lines demarcate the boundaries of the moments (start marked with 0).

4.4. DISCUSSION

In this study, we leveraged a unique combination of challenging behavioral, electrophysiological, and statistical approaches specifically to test whether the phenomenon of sequence replay observed for spatial information extends to other stimulus modalities and cognitive demands. We provide the first direct evidence of hippocampal replay for multi-step sequences of nonspatial and discontiguous states reflecting task-critical associations. Replay in the forward direction was prevalent during intervals preceding each event (odor) of the sequence and reactivated remaining parts of the sequence. In contrast, replay in the reverse direction was less frequent and primarily occurred after the end of the sequence. These findings suggest that

hippocampus can extract task-critical moments from extended continuous experiences, capture their sequential relationships, and rapidly replay them in the forward direction to evaluate potential mental steps leading to a goal or in reverse to consolidate or preserve learned representations.

The forward replay of spatial trajectories leading to a rewarded goal location is well documented in the literature (38, 41). Such replay, which can start locally (from the animal's current location; 38,137) or remotely (from another location; 106), typically reactivates the representations of the sequence of contiguous locations leading to a reward site. These observations are generally interpreted as reflecting a broader role for forward replay in planning upcoming behavior (i.e., beyond spatial navigation), a link that is now directly supported by our findings. Specifically, we observed local replays that started from the closest event in the sequence (i.e., the odor immediately before or after the interval) as well as remote replays that started with an event later in the sequence. Interestingly, our results also suggest a more nuanced characterization of the animals' goal than a rewarded site or action. The pattern of replay we observed suggests that the goal was the end of the sequence (i.e., the presentation of the last odor), as it was where forward replay ended and reverse replay began. Notably, animals received the same water reward after each odor presentation, so the last odor was not differentially rewarded. This suggests a goal representation that is not specifically tied to reward and is more conceptual in nature. Finally, spatial forward replay can also represent shortcuts to goals, highlighting its role in flexibly expressing spatial relationships within an environment. We view our replay of discontiguous task events (shortcutting time periods between them) as the expression of the same fundamental property of "navigating" the task representational space, in this case the set of non-spatial associations predicting successful performance.

Previous studies have shown that reverse replay is more prevalent in novel environments and tends to diminish as familiarity grows, highlighting its role in the initial learning of mental maps (103, 119, 124-125). Our results suggest the function of reverse replay goes beyond this initial learning. In fact, we observed reverse replay in animals tested on a familiar sequence when task rules were established and rewards consistently received for specific behaviors at specific locations. Our results indicate that reverse replay may also help reinforce learned associations that are important for task performance, aligning with the few studies showing reverse replay is also present in familiar environment and can represent paths to locations where animals have frequently received rewards. In our design, the presentation of out of sequence items, which are inconsistent with the learned representation of the sequence, may have promoted reverse replay dynamics as a mechanism to protect or maintain the learned representation against interfering events. Our results also suggest a more complex interpretation of the relationship between reverse replay and reward. Reverse replay moments primarily clustered in two intervals. As noted above, one interval was at the end of the sequence (after odor E), even though the amount of reward was the same for each odor in the sequence. The other interval was at the opposite end of the track, where the reward was larger, and replay counts generally (but not always) higher than at the end of the sequence (see Fig 5 and Suppl Fig 2). These results suggest reverse replay counts are not simply reflecting reward delivery or its magnitude and that other processes are involved to determine what constitutes a meaningful segment of experience to replay and what is the appropriate goal to represent in the task at hand.

Our results also prompt several important questions to address in future studies. When animals encounter a novel sequence within the same task, it is unclear how the content and direction of replay may change as they learn the correct sequence. Previous research suggests an

increase in reverse replay rates in new environments (103, 108, 111, 124-125), and we expect similar patterns here. However, to test this, we need to develop a statistical framework that accounts for the challenges of this task, such as fewer odor stimuli available for training classifiers due to anticipated early learning errors, or possibly using a setup where animals are previously exposed to the odors before starting the task. Our findings show that not all replay events coincide with SWR, consistent with previous studies reporting similar rates of coincidence (105-106, 137, 143, 162-164). Our results show that the LFP during replay events does not favor any specific frequency band compared to control events. But, further investigating the differences in LFP characteristics between replay events that overlap with SWR and those that don't, could reveal potential variations in their neural signatures. Our data indicate that replay sequences in both forward and reverse directions focus on odor E, marking it as a conceptual goal rather than a reward-related one, since each odor is followed by a reward. This highlights odor E as the final target within the sequence, and it would be intriguing to delve deeper into how replays that conclude at a conceptual goal differ from those oriented towards direct rewards, potentially revealing new insights into goal-directed behavior in animals. Our results suggest that replay mechanisms may create temporal shortcuts to goals by efficiently navigating through sequences. This observation opens new avenues for research into how animals integrate discrete and continuous aspects of tasks. Developing a statistical framework that can measure the replay of both the sequential moments of time within the sequence and the discrete events involved could provide further insight into the dynamics of memory replay and its role in learning and navigation.

In summary, the present study represents a significant advance in our understanding of sequence replay. By demonstrating how this phenomenon extends to other modalities and

captures more complex cognitive demands, our findings provide critical support for computational and theoretical proposals of a fundamental and broad role for hippocampal replay in learning, consolidating, and retrieving multi-step associations to guide goal-directed decisions.

CHAPTER 5: SUMMARY

In this thesis, I aimed to develop a better understanding of the neural mechanisms with which hippocampal activity supports the memory of the order of events in a sequence. Specifically, I investigated whether the sequence generating property of CA1 ensembles supports the memory of discrete events separated in time, akin to daily life episodes. To do so, I leveraged our labs existing CA1 dataset recorded as animals are engaged in a demanding non-spatial sequence memory task, which mirrors our daily life episodes by incorporating a series of discontiguous odor presentations separated by rest intervals. Next, I built statistical frameworks designed to quantify distinct sequence coding properties (i.e., time cell activity and hippocampal replay) during discrete task events. Importantly, the task design and the frameworks enabled us to determine if CA1 ensembles exhibit unique sequence coding properties and get deeper insights into their specific roles and distribution during different moments in the task.

5.1. SUMMARY OF TEMPORAL CODING IN THE CA1 ENSEBLES (CHAPTER 2)

In this chapter, I investigated whether sequential firing fields (i.e., time cell activity) support the temporal organization of events that are widely separated in time, a fundamental feature of our daily experiences. While the sequential firing fields are known to provide a temporal signal during individual task events (46, 48, 54, 89-94), it remains unclear whether they also enhance the hippocampus's ability to organize discontiguous events in time. To test this, I visualized the sequential firing field activity using PSTHs and quantified temporal coding strength of the ensemble activity using a Bayesian model. Briefly, the model yielded probability

distributions of reconstructed times for specific task events, enabling us to assess temporal coding accuracy by evaluating how accurately time was reconstructed within these events.

Our findings strongly indicate that sequential firing fields could serve as a mechanism through which the hippocampus supports memory for order of events in a sequence. Specifically, we observed that the CA1 ensembles exhibited sequential firing fields during stimulus presentation, which are stimulus-specific, and provide with strong temporal coding during these events (Fig 2.3). This chapter also examined whether temporal coding accuracy changes based on the temporal distance between odor presentations (in terms of the position in sequence; lag). Our findings support the temporal context model (82), demonstrating that temporal coding accuracy varies by lag, being highest at a lag of 0 and decreasing linearly as the lag increases. Interestingly, even though accuracy decreases with increasing lag, it remains significantly above chance levels for all lags. This suggests that the temporal organization of stimuli is partially shared and varies with lag, such that the temporal distance between stimuli is reflected by the degree of dissimilarity of their neural activity (Fig 2.5). This chapter also investigated whether sequential firing fields bridges across sequences of stimuli and the intervals in between, lasting throughout entire sequence presentation. Despite variations in individual odor timings, we found sequential organization of firing fields across the full sequence (~25 seconds), which also provided with strong temporal coding accuracy across this entire duration (Fig 2.6). Collectively, the results suggest that the sequential firing field activity of the CA1 ensembles provide strong temporal signal that encodes information about the identity of individual stimuli, their position in a sequence, and bridges across a series of stimuli presentations.

5.2. SUMMARY OF STATISTICAL FRAMEWORK TO QUANTIFY SEQUENCE REPLAY OF DISCRETE NONSPATIAL STATES (CHAPTER 3)

In this chapter, I outlined the development a statistical framework designed to evaluate sequence replay predictions involving the replay of temporally separated discrete events (discussed in chapter 4). The need for a new statistical framework arose because existing models are primarily suited to determine replay of sequences of continuous states, like spatial locations, and depend heavily on the replay of place cells, which are more straightforward to detect compared to patterns in ensemble activity representing temporally separated events (106, 138-141, 147). Specifically, we developed a framework capable of identifying replay moments during awake resting periods (i.e., during the intervals) and determined whether the content, direction and distribution of the replay moments matched our predicted patterns.

We built this framework by adapting the sequenceness metric, previously used for quantifying replay of nonspatial events in MEG data (90-91), and further expanded this metric to allow us to determine the exact order of replayed odors during replay moments, visualize the activity of individual cells during these moments, and assess whether the replayed content and direction changes based on the interval type (i.e., animals' temporal location in the sequence with respect to its goal). Additionally, we determined the essential parameters of the framework based on CA1 activity, which are crucial to test our sequence replay predictions (Fig 3.2, 3.3). The critical outputs of this framework are the regression coefficients (i.e., β's), which measure the likelihood of replaying any two adjacent odor pairs within 25 ms bins during intervals (e.g., βCD for the replay of odor C followed by D). We computed consecutive β's from these individual β's to quantify the replay of sequences of 2+ odors (e.g., βCDE for the replay of odors C, D, and E). By utilizing both individual and consecutive β's, we identified significant replay moments during the

intervals (e.g., a replay moment of odors A-E in the forward direction is marked by significant βABCDE). Once the framework was built, we analyzed CA1 ensembles to obtain essential parameters of the framework before testing it to check our sequence replay predictions. First, we determined the optimal time window during odor presentation to train our classifier, which we identified as 300-500 ms period post nose poke-in (Fig 3.2). Secondly, we assessed the incorporation of a null state to control for multicollinearity, a potential problem when conducting time-lagged regressions on odor probabilities (Fig 3.2 C). Importantly, adding the null state did not impact the performance of the classifier. Lastly, we determined the optimal time lag (Δt; Fig 3.3) reflecting the time lag between bins within replay moments (longer Δt would mean longer duration of replay moments for the same replayed content). We found the optimal Δt to be 25 ms which we fixed to test our sequence replay predictions in chapter 4.

5.3. SUMMARY OF HIPPOCAMPAL SEQUENCE REPLAY OF DISCRETE NONSPATIAL STATES (CHAPTER 4)

Hippocampal replay is associated with numerous fundamental cognitive processes and serves as evidence of the hippocampus's ability to generate sequences, a capacity known to support the memory of the order of events in a sequence (55-59). However, it remains unclear whether this phenomenon extends to other stimulus modalities and task demands, especially in organizing discrete events separated in time. In this chapter, I investigated whether the hippocampal sequence replay phenomenon, observed for spatial information, also applies to nonspatial information involving discontiguous stimuli. To determine this, I utilized the framework established in chapter 3 and tested our working model of predicted distributions of replay moments across intervals (Fig 4.1).

We presented the first direct evidence of hippocampal replay for multi-step sequences of nonspatial and discontiguous states that reflect task-critical associations. Specifically, our findings are in line with the spatial replay literature (39, 90, 137) and extend the replay phenomenon to complex sequential relationships across discrete events by demonstrating the replay of odor sequences during moments in the intervals. We observed that forward replay reflects the animal's expectations for upcoming parts of the sequence where the replay moments represented upcoming steps to the goal (Fig 4.2). For example, βABCDE moments were significantly more prevalent in the first interval (interval after odor A), βBCDE moments in the first two intervals (before and after B), βCDE in the first three intervals, and βDE in the first four intervals. Interestingly, such forward replay either started locally (with the closest odor) or remotely from a future sequence position, but *not* from a remote past sequence position (e.g., BCDE when adjacent to D) nor after completion of the sequence (after E). Importantly, the replay moments ended at odor E, which is the goal and is not differently rewarded but is more conceptual in nature as it marks the end of the sequence. Unlike the pattern observed with forward replay, we observed that reverse replay is stronger at the end of the sequence (i.e., once the goal has been reached), that is both after odor E and after the larger reward is consumed at the other end of the track (Fig 4.6). Specifically, we observed that consecutive odor sequences were replayed in reverse after the end of the sequence presentation. Where, βEDCBA, βDCBA, βCBA, and βBA moments were significantly more prevalent in the two intervals after odor E presentation (except for βEDCBA counts being high before odor E). Together, these results highlight the unique roles of forward and reverse replay moments in meeting the requirements of our sequence memory paradigm. They suggest that forward replay helps evaluate potential sequences of states that are more abstract or associative goals (i.e., odor E in our task).

Furthermore, the findings also indicate that the role of reverse replay extends beyond forming and consolidating new learning and includes maintaining learned representations of goal related sequences.

5.4. GENERAL DISCUSSION

In chapters 2-4 we investigated distinct sequence coding mechanisms in the CA1 ensembles and their specific roles when the animals are engaged in our nonspatial sequence memory paradigm. Importantly, we provided direct evidence of time cell activity and hippocampal replay during behavior and showed that both these distinct sequence coding mechanisms occur within the same CA1 recordings of the same animals engaged in the same task. Specifically, we demonstrated that these distinct phenomena unfold at different times during behavior, with time cell activity unfolding during individual task events and hippocampal replay during intervals separating them. Our research offers further insights into the unique functions of these mechanisms. Time cell activity captures the sequential relationship among stimuli and provides a continuous temporal signal throughout the sequence, which includes both the odor presentations and the intervals separating them. In contrast, replay captures only the essential task information, specifically by representing only odor identities without the intervals. Overall, our findings suggest that distinct sequence coding phenomena are active at different times during the task, and that these mechanisms could be supporting distinct aspects needed for temporally organizing memories. Our findings also support the idea that the hippocampal network's capacity to create and maintain sequential activity patterns is crucial for its ability to support sequence memory (55-59).

Collectively, our findings prompt interesting avenues to expand this work. In addition to the time cell and hippocampal replay presented in this thesis, other sequence coding mechanisms are also linked to temporally organizing experiences. Similar to hippocampal replay, theta representations are shown crucial for planning and decision-making, as they maintain an online trajectory towards the current goal (153-154). Analysis of the same CA1 dataset shows that past, present, and future events are sequentially organized within theta cycles during stimulus presentations, which is associated with decision accuracy and trial-specific contingencies (153). These results show that these three coding mechanisms represent overlapping information which suggests that their roles may be interconnected. Specifically, within the same CA1 dataset, sequence replay and theta cycles represent task-critical information (i.e., odor identities without the intervals), time cell activity and theta reflect correct order memory judgements, and all the three mechanisms represent sequential relationships among odors in different ways. To further explore how the hippocampus supports the temporal organization of memories, it will be valuable to investigate the relationship between these coding mechanisms, assess their unique contributions, and understand how they collectively facilitate memory of sequences of events.

Investigating how these mechanisms affect behavioral decisions and examining the role of other brain regions, is crucial for understanding how the brain supports sequence memory. The prefrontal cortex is particularly significant in this context. Numerous studies have demonstrated the significant role of the prefrontal cortex and its interaction with the hippocampus in organizing temporal experiences across species. For example, fMRI studies show activation in both regions during the encoding and retrieval of temporal information (21-24). Similarly, studies on the primate dorsolateral and ventrolateral prefrontal cortex reveal time cell activity during nonspatial tasks, indicating that this temporal structure might be a

fundamental organizing principle in various brain regions (152). Further evidence shows that the prefrontal cortex can rapidly reactivate task-related information, like the hippocampus (41). These tend to coincide with SWRs and occur during low voltage spindles of 10-20 Hz and delta oscillations of 0.1-4 Hz in slow wave sleep (118, 134-135), as well as during wakefulness, where specific groups of prefrontal neurons are selectively excited or inhibited (134). Despite recognizing the involvement of the prefrontal cortex, its distinct neurobiological mechanisms and interactions with hippocampus in supporting sequence memory are less understood. To investigate this, simultaneous recordings from these brain structures are necessary while animals are engaged in a nonspatial sequence memory task. Combining these recordings with optogenetic techniques to inactivate specific regions can help further test their behavioral influence and distinct contributions.

REFERENCES

1. Mauk, M. D., & Buonomano, D. V. (2004). The neural basis of temporal processing. Annual Review of Neuroscience, 27, 307-340.

2. Buhusi, C. V., & Meck, W. H. (2005). What makes us tick? Functional and neural mechanisms of interval timing. Nature Reviews Neuroscience, 6, 755-765.

3. Allen, T. A., & Fortin, N. J. (2013). The evolution of episodic memory. Proceedings of the National Academy of Sciences, 110, 10379-10386.

4. Merchant, H., Harrington, D. L., & Meck, W. H. (2013). Neural basis of the perception and estimation of time. Annual Review of Neuroscience, 36, 313-336.

5. Tulving, E. (1972). Episodic and semantic memory. In E. Tulving & W. Donaldson (Eds.), Organization of Memory (pp. 381-403). Academic Press.

6. Griffiths, D., Dickinson, A., & Clayton, N. (1999). Episodic memory: What can animals remember about their past? Trends in Cognitive Sciences, 3(2), 74-80.

7. Eichenbaum, H., & Fortin, N. J. (2005). Bridging the gap between brain and behavior: Cognitive and neural mechanisms of episodic memory. Journal of the Experimental Analysis of Behavior, 84, 619-629.

8. Crystal, J. D. (2009). Elements of episodic-like memory in animal models. Behavioural Processes, 80, 269-277.

9. Ranganath, C., & Ritchey, M. (2012). Two cortical systems for memory-guided behavior. Nature Reviews Neuroscience, 13, 713-726.

10. Eichenbaum, H. (2014). Time cells in the hippocampus: A new dimension for mapping memories. Nature Reviews Neuroscience, 15, 732-744.

11. Davachi, L., & DuBrow, S. (2015). How the hippocampus preserves order: The role of prediction and context. Trends in Cognitive Sciences, 19, 92-99.

12. Allen, T. A., Morris, A. M., Stark, S. M., Fortin, N. J., & Stark, C. E. (2015). Memory for sequences of events impaired in typical aging. Learning & Memory, 22(3), 138-148.

13. Pause, B. M., Zlomuzica, A., Kinugawa, K., Mariani, J., Pietrowsky, R., & Dere, E. (2013). Perspectives on episodic-like and episodic memory. Frontiers in Behavioral Neuroscience, 7, 33.

14. Durand, T., Berzero, G., Bompaire, F., Hoffmann, S., Léger, I., Jego, V., Baruteau, M., Delgadillo, D., Taillia, H., Psimaras, D., & Ricard, D. (2018). Episodic memory impairments in primary brain tumor patients. Archives of Clinical Neuropsychology, 33(8), 949-955.

15. Fortin, N. J., Agster, K. L., & Eichenbaum, H. B. (2002). Critical role of the hippocampus in memory for sequences of events. Nature Neuroscience, 5(5), 458-462.

16. Kesner, R. P., Gilbert, P. E., & Barua, L. A. (2002). The role of the hippocampus in memory for the temporal order of a sequence of odors. Behavioral Neuroscience, 116(2), 286-290.

17. Chiba, A. A., Kesner, R. P., & Reynolds, A. M. (1994). Memory for spatial location as a function of temporal lag in rats: Role of hippocampus and medial prefrontal cortex. Behavioral and Neural Biology, 61, 123-131.

18. Spiers, H. J., Burgess, N., Hartley, T., Vargha-Khadem, F., & O'Keefe, J. (2001). Bilateral hippocampal pathology impairs topographical and episodic memory but not visual pattern matching. Hippocampus, 11(6), 715-725.

19. Downes, J. J., Mayes, A. R., MacDonald, C., & Hunkin, N. M. (2002). Temporal order memory in patients with Korsakoff's syndrome and medial temporal amnesia. Neuropsychologia, 40(7), 853-861.

20. Naya, Y., & Suzuki, W. A. (2011). Integrating what and when across the primate medial temporal lobe. Science, 333, 773-776.

21. Reeders, P. C., Hamm, A. G., Allen, T. A., & Mattfeld, A. T. (2021). Medial prefrontal cortex and hippocampal activity differentially contribute to ordinal and temporal context retrieval during sequence memory. Learning & Memory, 28(4), 134-147.

22. Ekstrom, A. D., & Bookheimer, S. Y. (2007). Spatial and temporal episodic memory retrieval recruit dissociable functional networks in the human brain. Learning & Memory, 14, 645-654.

23. Jenkins, L. J., & Ranganath, C. (2010). Prefrontal and medial temporal lobe activity at encoding predicts temporal context memory. Journal of Neuroscience, 30, 15558-15565.

24. Kumaran, D., & Maguire, E. A. (2006). An unexpected sequence of events: Mismatch detection in the human hippocampus. PLoS Biology, 4(12), e424.

25. Hsieh, L. T., Gruber, M. J., Jenkins, L. J., & Ranganath, C. (2014). Hippocampal activity patterns carry information about objects in temporal context. Neuron, 81, 1165-1178.

26. Ezzyat, Y., & Davachi, L. (2014). Similarity breeds proximity: Pattern similarity within and across contexts is related to mnemonic judgments of temporal proximity. Neuron, 81, 1179-1189.

27. Pastalkova, E., Itskov, V., Amarasingham, A., & Buzsaki, G. (2008). Internally generated cell assembly sequences in the rat hippocampus. Science, 321, 1322-1327.

28. MacDonald, C. J., Lepage, K. Q., Eden, U. T., & Eichenbaum, H. (2011). Hippocampal 'time cells' bridge the gap in memory for discontiguous events. Neuron, 71, 737-749.

29. Tiganj, Z., Jung, M. W., Kim, J., & Howard, M. W. (2017). Sequential firing codes for time in rodent medial prefrontal cortex. Cerebral Cortex, 27(12), 5663-5671.

30. Aronov, D., Nevers, R., & Tank, D. W. (2017). Mapping of a non-spatial dimension by the hippocampal-entorhinal circuit. Nature, 543, 719-722.

31. McNaughton, B. L., & Morris, R. G. (1987). Hippocampal synaptic enhancement and information storage within a distributed memory system. Trends in Neurosciences, 10(10), 408-415.

32. Levy, B. (1996). Improving memory in old age through implicit self-stereotyping. Journal of Personality and Social Psychology, 71(6), 1092-1107.

33. Tsodyks, M. V., Skaggs, W. E., Sejnowski, T. J., & McNaughton, B. L. (1996). Population dynamics and theta rhythm phase precession of hippocampal place cell firing: A spiking neuron model. Hippocampus, 6(3), 271-280.

34. Lisman, J. E. (1999). Relating hippocampal circuitry to function: Recall of memory sequences by reciprocal dentate–CA3 interactions. Neuron, 22(2), 233-242.

35. Howard, M. W., & Natu, V. S. (2005). Place from time: Reconstructing position from a distributed representation of temporal context. Neural Networks, 18(9), 1150-1162.

36. Howard, M. W., MacDonald, C. J., Tiganj, Z., Shankar, K. H., Du, Q., Hasselmo, M. E., & Eichenbaum, H. (2014). A unified mathematical framework for coding time, space, and sequences in the hippocampal region. Journal of Neuroscience, 34(13), 4692-4707.

37. Foster, D. J., & Knierim, J. J. (2012). Sequence learning and the role of the hippocampus in rodent navigation. Current Opinion in Neurobiology, 22(2), 294-300.

38. Davidson, T. J., Kloosterman, F., & Wilson, M. A. (2009). Hippocampal replay of extended experience. Neuron, 63, 497-507.

39. Diba, K., & Buzsáki, G. (2007). Forward and reverse hippocampal place-cell sequences during ripples. Nature Neuroscience, 10, 1241-1242.

40. Foster, D. J. (2017). Replay comes of age. Annual Review of Neuroscience, 40, 581-602.

41. Joo, H. R., & Frank, L. M. (2018). The hippocampal sharp wave–ripple in memory retrieval for immediate use and consolidation. Nature Reviews Neuroscience, 19, 744-757.

42. Hannesson, D. K., Howland, J. G., & Phillips, A. G. (2004). Interaction between perirhinal and medial prefrontal cortex is required for temporal order but not recognition memory for objects in rats. Journal of Neuroscience, 24(19), 4596-4604.

43. Hatakeyama, T., Sugita, M., Yamada, K., & Ichitani, Y. (2018). Temporal order memory of the rat in spontaneous object recognition: Effects of number of items, exposure interval, and retention time. Learning & Memory, 25(11), 574-579.

44. Milner, B., Petrides, M., & Smith, M. L. (1985). Frontal lobes and the temporal organization of memory. Human Neurobiology, 4(3), 137-142.

45. Eichenbaum, H. (2017). Time (and space) in the hippocampus. Current Opinion in Behavioral Sciences, 17, 65-70.

46. Allen, T. A., Morris, A. M., Mattfeld, A. T., Stark, C. E., & Fortin, N. J. (2014). A sequence of events model of episodic memory shows parallels in rats and humans. Hippocampus, 24(10), 1178-1188.

47. Shankar, K. H., & Howard, M. W. (2010). Timing using temporal context. Brain Research, 1365, 3-17.

48. Terada, S., Sakurai, Y., Nakahara, H., & Fujisawa, S. (2017). Temporal and rate coding for discrete event sequences in the hippocampus. Neuron, 94, 1248-1262.

49. Eichenbaum, H., Otto, T., & Cohen, N. J. (1994). Two functional components of the hippocampal memory system. Behavioral and Brain Sciences, 17, 449-472.

50. Rawlins, J. N. P. (1985). Associations across time: The hippocampus as a temporary memory store. Behavioral and Brain Sciences, 8, 479-496.

51. Kesner, R. P., Hunsaker, M. R., & Ziegler, W. (2010). The role of the dorsal CA1 and ventral CA1 in memory for the temporal order of a sequence of odors. Neurobiology of Learning and Memory, 93(1), 111-116.

52. Fyhn, M., Molden, S., Hollup, S., Moser, M. B., & Moser, E. (2002). Hippocampal neurons responding to first-time dislocation of a target object. Neuron, 35, 555-566.

53. Lehn, H., Steffenach, H. A., van Strien, N. M., Veltman, D. J., Witter, M. P., & Håberg, A. K. (2009). A specific role of the human hippocampus in recall of temporal sequences. Journal of Neuroscience, 29(11), 3475-3484.

54. Ross, R. S., Brown, T. I., & Stern, C. E. (2009). The retrieval of learned sequences engages the hippocampus: Evidence from fMRI. Hippocampus, 19(9), 790-799.

55. Redish, A. D. (2016). Vicarious trial and error. Nature Reviews Neuroscience, 17, 147-159.

56. Lisman, J. E., & Redish, A. D. (2009). Prediction, sequences and the hippocampus. Philosophical Transactions of the Royal Society B: Biological Sciences, 364, 1193-1201.

57. Levy, W. B. (1996). A sequence predicting CA3 is a flexible associator that learns and uses context to solve hippocampal-like tasks. Hippocampus, 6, 579-590.

58. Buzsáki, G., & Tingley, D. (2018). Space and time: The hippocampus as a sequence generator. Trends in Cognitive Sciences, 22(10), 853-869.

59. Buckner, R. L. (2010). The role of the hippocampus in prediction and imagination. Annual Review of Psychology, 61(1), 27-48.

60. Allen, T. A., Salz, D. M., McKenzie, S., & Fortin, N. J. (2016). Nonspatial sequence coding in CA1 neurons. Journal of Neuroscience, 36(5), 1547-1563.

61. Montchal, M. E., Reagh, Z. M., & Yassa, M. A. (2019). Precise temporal memories are supported by the lateral entorhinal cortex in humans. Nature Neuroscience, 22, 284-288.

62. Ranganath, C., & Hsieh, L. T. (2016). The hippocampus: A special place for time. Annals of the New York Academy of Sciences, 1369, 93-110.

63. Mankin, E. A., Sparks, F. T., Slayyeh, B., Sutherland, R. J., Leutgeb, S., & Leutgeb, J. K. (2012). Neuronal code for extended time in the hippocampus. Proceedings of the National Academy of Sciences, 109(47), 19462-19467.

64. Manns, J. R., Howard, M. W., & Eichenbaum, H. (2007). Gradual changes in hippocampal activity support remembering the order of events. Neuron, 56(3), 530-540.

65. Chen, Z. S., & Wilson, M. A. (2023). How our understanding of memory replay evolves. Journal of Neurophysiology, 129(3), 552-580.

66. Nitzan, N., Swanson, R., Schmitz, D., & Buzsáki, G. (2022). Brain-wide interactions during hippocampal sharp wave ripples. Proceedings of the National Academy of Sciences, 119(20), e2200931119.

67. Schapiro, A. C., McDevitt, E. A., Rogers, T. T., Mednick, S. C., & Norman, K. A. (2018). Human hippocampal replay during rest prioritizes weakly learned information and predicts memory performance. Nature Communications, 9(1), 3920.

68. Tulving, E., & Markowitsch, H. J. (1998). Episodic and declarative memory: Role of the hippocampus. Hippocampus, 8(3), 198-204.

69. Tsao, A., et al. (2018). Integrating time from experience in the lateral entorhinal cortex. Nature, 561, 57-62.

70. McKenzie, S., et al. (2016). Representation of memories in the cortical–hippocampal system: Results from the application of population similarity analyses. Neurobiology of Learning and Memory, 134, 178-191.

71. Bright, I. M., Meister, M. L. R., Cruzado, N. A., Tiganj, Z., Buffalo, E. A., & Howard, M. W. (2020). A temporal record of the past with a spectrum of time constants in the monkey entorhinal cortex. Proceedings of the National Academy of Sciences, 117(33), 20274-20283.

72. O'Keefe, J., & Dostrovsky, J. (1971). The hippocampus as a spatial map. Preliminary evidence from unit activity in the freely-moving rat. Brain Research, 34, 171-175.

73. Wilson, M. A., & McNaughton, B. L. (1993). Dynamics of the hippocampal ensemble code for space. Science, 261, 1055-1058.

74. MacDonald, C. J., Carrow, S., Place, R., & Eichenbaum, H. (2013). Distinct hippocampal time cell sequences represent odor memories in immobilized rats. Journal of Neuroscience, 33(35), 14607-14616.

75. Salz, D. M., et al. (2016). Time cells in hippocampal area CA3. Journal of Neuroscience, 36, 7476-7484.

76. Kraus, B. J., et al. (2015). During running in place, grid cells integrate elapsed time and distance run. Neuron, 88, 578-589.

77. Clewett, D., DuBrow, S., & Davachi, L. (2019). Transcending time in the brain: How event memories are constructed from experience. Hippocampus, 29, 162-183.

78. Bright, I. M. (2023). A scale-invariant representation of temporal context: Support and constraints from neural and behavioral data. Boston University (Doctoral dissertation).

79. Modi, M. N., Dhawale, A. K., & Bhalla, U. S. (2014). CA1 cell activity sequences emerge after reorganization of network correlation structure during associative learning. eLife, 3, e01982.

80. Sakon, J. J., et al. (2014). Context-dependent incremental timing cells in the primate hippocampus. Proceedings of the National Academy of Sciences, 111, 18351-18356.

81. Umbach, G., Kantak, P., Jacobs, J., Kahana, M. J., Pfeiffer, B. E., Sperling, M., & Lega, B. (2020). Time cells in the human hippocampus and entorhinal cortex support episodic memory. Proceedings of the National Academy of Sciences, 117(45), 28463-28474.

82. Howard, M. W., & Kahana, M. J. (2002). A distributed representation of temporal context. Journal of Mathematical Psychology, 46(3), 269-299.

83. Sederberg, P. B., Howard, M. W., & Kahana, M. J. (2008). A context-based theory of recency and contiguity in free recall. Psychological Review, 115(4), 893-912.

84. Usher, M., & McClelland, J. L. (2001). The time course of perceptual choice: The leaky, competing accumulator model. Psychological Review, 108(3), 550-592.

85. Howard, M. W., Kahana, M. J., & Wingfield, A. (2006). Aging and contextual binding: Modeling recency and lag recency effects with the temporal context model. Psychonomic Bulletin & Review, 13(3), 439-445.

86. Shankar, K. H., & Howard, M. W. (2012). A scale-invariant internal representation of time. Neural Computation, 24(1), 134-193.

87. Liu, Y., Tiganj, Z., Hasselmo, M. E., & Howard, M. W. (2019). A neural microcircuit model for a scalable scale-invariant representation of time. Hippocampus, 29(3), 260-274.

88. Howard, M. W., Fotedar, M. S., Datey, A. V., & Hasselmo, M. E. (2005). The temporal context model in spatial navigation and relational learning: Toward a common explanation of medial temporal lobe function across domains. Psychological Review, 112(1), 75-116.

89. Aggleton, J. P., & Brown, M. W. (1999). Episodic memory, amnesia, and the hippocampal-anterior thalamic axis. Behavioral and Brain Sciences, 22, 425-489.

90. Liu, Y., Dolan, R. J., & Kurth-Nelson, Z., & Behrens, T. E. J. (2019). Human replay spontaneously reorganizes experience. Cell, 178(3), 649-662.

91. Liu, Y., Dolan, R. J., Higgins, C., Penagos, H., Woolrich, M. W., Ólafsdóttir, H. F., Barry, C., Kurth-Nelson, Z., & Behrens, T. E. J. (2021). Temporally delayed linear modelling (TDLM) measures replay in both animals and humans. eLife, 10, e66917.

92. Fortin, N. J., Agster, K. L., & Eichenbaum, H. B. (2016). Distinct contributions of hippocampal, prefrontal, perirhinal, and nucleus reuniens regions to the memory for sequences of events. In Society for Neuroscience Abstracts.

93. Boucquey, V. K., Allen, T. A., Huffman, D. J., Fortin, N. J., & Stark, C. E. L. (n.d.). A cross-species sequence memory task reveals hippocampus and medial prefrontal cortex activity and interactions in humans. SfN Abstract (Chicago, IL). Manuscript under revision.

94. Zhang, K., Ginzburg, I., McNaughton, B. L., & Sejnowski, T. J. (1998). Interpreting neuronal population activity by reconstruction: Unified framework with application to hippocampal place cells. Journal of Neurophysiology, 79, 1017-1044.

95. Brown, M. W., & Aggleton, J. P. (2001). Recognition memory: What are the roles of the perirhinal cortex and hippocampus? Nature Reviews Neuroscience, 2, 51-61.

96. Murray, E. A., & Bussey, T. J. (1999). Perceptual-mnemonic functions of the perirhinal cortex. Trends in Cognitive Sciences, 3, 142-151.

97. Gaffan, D. (1994). Dissociated effects of perirhinal cortex ablation, fornix transection and amygdalectomy: Evidence for multiple memory systems in the primate temporal lobe. Experimental Brain Research, 99, 411-422.

98. Manns, J. R., & Eichenbaum, H. (2006). Evolution of declarative memory. Hippocampus, 16(9), 795-808.

99. Amaral, D. G., & Witter, M. P. (1989). The three-dimensional organization of the hippocampal formation: A review of anatomical data. Neuroscience, 31(3), 571-591.

100. van Strien, N. M., Cappaert, N. L., & Witter, M. P. (2009). The anatomy of memory: An interactive overview of the parahippocampal-hippocampal network. Nature Reviews Neuroscience, 10(4), 272-282.

101. Insausti, R. (1993). Comparative anatomy of the entorhinal cortex and hippocampus in mammals. Hippocampus, 3(Special Issue), 19-26.

102. Witter, M. P., Wouterlood, F. G., Naber, P. A., & Van Haeften, T. (2000). Anatomical organization of the parahippocampal-hippocampal network. Annals of the New York Academy of Sciences, 911, 1-24.

103. Carr, M. F., Jadhav, S. P., & Frank, L. M. (2011). Hippocampal replay in the awake state: A potential substrate for memory consolidation and retrieval. Nature Neuroscience, 14(2), 147-153.

104. Buzsáki, G. (2015). Hippocampal sharp wave-ripple: A cognitive biomarker for episodic memory and planning. Hippocampus, 25(10), 1073-1188.

105. Pfeiffer, B. E., & Foster, D. J. (2013). Hippocampal place-cell sequences depict future paths to remembered goals. Nature, 497, 74-79.

106. Karlsson, M., & Frank, L. (2009). Awake replay of remote experiences in the hippocampus. Nature Neuroscience, 12, 913-918.

107. Bhattarai, B., Lee, J. W., & Jung, M. W. (2020). Distinct effects of reward and navigation history on hippocampal forward and reverse replays. Proceedings of the National Academy of Sciences, 117(1), 689-697.

108. Singer, A. C., Carr, M. F., Karlsson, M. P., & Frank, L. M. (2013). Hippocampal SWR activity predicts correct decisions during the initial learning of an alternation task. Neuron, 77, 1163-1173.

109. Foster, D. J., & Wilson, M. A. (2006). Reverse replay of behavioural sequences in hippocampal place cells during the awake state. Nature, 440, 680-683.

110. O'Neill, J., Pleydell-Bouverie, B., Dupret, D., & Csicsvari, J. (2010). Play it again: Reactivation of waking experience and memory. Trends in Neurosciences, 33, 220-229.

111. Dupret, D., O'Neill, J., Pleydell-Bouverie, B., & Csicsvari, J. (2010). The reorganization and reactivation of hippocampal maps predict spatial memory performance. Nature Neuroscience, 13(8), 995-1002.

112. Girardeau, G., Benchenane, K., Wiener, S. I., Buzsaki, G., & Zugaro, M. B. (2009). Selective suppression of hippocampal ripples impairs spatial memory. Nature Neuroscience, 12, 1222-1223.

113. Ego-Stengel, V., & Wilson, M. A. (2010). Disruption of ripple-associated hippocampal activity during rest impairs spatial learning in the rat. Hippocampus, 20(1), 1-10.

114. Wilson, M. A., & McNaughton, B. L. (1994). Reactivation of hippocampal ensemble memories during sleep. Science, 265, 676-679.

115. Jadhav, S. P., Kemere, C., German, P. W., & Frank, L. M. (2012). Awake hippocampal sharp-wave ripples support spatial memory. Science, 336, 1454-1458.

116. Singer, A. C., & Frank, L. M. (2009). Rewarded outcomes enhance reactivation of experience in the hippocampus. Neuron, 64(6), 910-921.

117. Ólafsdóttir, H. F., Bush, D., & Barry, C. (2018). The role of hippocampal replay in memory and planning. Current Biology, 28(1), R37-R50.

118. Shin, J. D., Tang, W., & Jadhav, S. P. (2019). Dynamics of awake hippocampal-prefrontal replay for spatial learning and memory-guided decision making. Neuron, 104(6), 1110-1125.e7.

119. Gupta, A. S., van der Meer, M. A., Touretzky, D. S., & Redish, A. D. (2010). Hippocampal replay is not a simple function of experience. Neuron, 65(5), 695-705.

120. Csicsvari, J., O'Neill, J., Allen, K., & Senior, T. (2007). Place-selective firing contributes to the reverse-order reactivation of CA1 pyramidal cells during sharp waves in open-field exploration. European Journal of Neuroscience, 26(3), 704-716.

121. Berners-Lee, A., Feng, T., Silva, D., Wu, X., Ambrose, E. R., Pfeiffer, B. E., & Foster, D. J. (2022). Hippocampal replays appear after a single experience and incorporate greater detail with more experience. Neuron, 110(11), 1829-1842.

122. Xu, H., Baracskay, P., O'Neill, J., & Csicsvari, J. (2019). Assembly responses of hippocampal CA1 place cells predict learned behavior in goal-directed spatial tasks on the radial eight-arm maze. Neuron, 101(1), 119-132.e4.

123. Wirth, S., Avsar, E., Chiu, C. C., Sharma, V., Smith, A. C., Brown, E., & Suzuki, W. A. (2009). Trial outcome and associative learning signals in the monkey hippocampus. Neuron, 61, 930-940.

124. Roux, L., Hu, B., Eichler, R., Stark, E., & Buzsáki, G. (2017). Sharp wave ripples during learning stabilize the hippocampal spatial map. Nature Neuroscience, 20(6), 845-853.

125. Cheng, S., & Frank, L. M. (2008). New experiences enhance coordinated neural activity in the hippocampus. Neuron, 57, 303-313.

126. Roumis, D. K., & Frank, L. M. (2015). Hippocampal sharp-wave ripples in waking and sleeping states. Current Opinion in Neurobiology, 35, 6-12.

127. Buzsáki, G., Horváth, Z., Urioste, R., Hetke, J., & Wise, K. (1992). High-frequency network oscillation in the hippocampus. Science, 256(5059), 1025-1027.

128. Suzuki, S. S., & Smith, G. K. (1987). Spontaneous EEG spikes in the normal hippocampus. I. Behavioral correlates, laminar profiles and bilateral synchrony. Electroencephalography and Clinical Neurophysiology, 67(4), 348-359.

129. Kanamori, N. (1985). A spindle-like wave in the cat hippocampus: A novel vigilance level-dependent electrical activity. Brain Research, 334(1), 180-182.

130. Skaggs, W. E., & McNaughton, B. L. (1996). Replay of neuronal firing sequences in rat hippocampus during sleep following spatial experience. Science, 271(5257), 1870-1873.

131. Nádasdy, Z., Hirase, H., Czurkó, A., Csicsvari, J., & Buzsáki, G. (1999). Replay and time compression of recurring spike sequences in the hippocampus.

Journal of Neuroscience, 19(21), 9497-9507.

132. Lee, A. K., & Wilson, M. A. (2002). Memory of sequential experience in the hippocampus during slow wave sleep. Neuron, 36(6), 1183-1194.

133. Findlay, G., Tononi, G., & Cirelli, C. (2021). The evolving view of replay and its functions in wake and sleep. Sleep Advances, 1(1), zpab002.

134. Tang, W., Shin, J. D., Frank, L. M., & Jadhav, S. P. (2017). Hippocampal-prefrontal reactivation during learning is stronger in awake compared with sleep states. Journal of Neuroscience, 37(49), 11789-11805.

135. Peyrache, A., Khamassi, M., Benchenane, K., et al. (2009). Replay of rule-learning related neural patterns in the prefrontal cortex during sleep. Nature Neuroscience, 12, 919-926.

136. Fernández-Ruiz, A., Oliva, A., Fermino de Oliveira, E., Rocha-Almeida, F., Tingley, D., & Buzsáki, G. (2019). Long-duration hippocampal sharp wave ripples improve memory. Science, 364(6445), 1082-1086.

137. Widloski, J., & Foster, D. J. (2022). Flexible rerouting of hippocampal replay sequences around changing barriers in the absence of global place field remapping. Neuron, 110(9), 1547-1558.e8.

138. Yu, J. Y., Liu, D. F., Loback, A., Grossrubatscher, I., & Frank, L. M. (2018). Specific hippocampal representations are linked to generalized cortical representations in memory. Nature Communications, 9(1), 2209.

139. Gillespie, A. K., Astudillo Maya, D. A., Denovellis, E. L., Liu, D. F., Kastner, D. B., Coulter, M. E., Roumis, D. K., Eden, U. T., & Frank, L. M. (2021). Hippocampal replay reflects specific past experiences rather than a plan for subsequent choice. Neuron, 109(19), 3149-3163.e6.

140. Denovellis, E. L., Gillespie, A. K., Coulter, M. E., Sosa, M., Chung, J. E., Eden, U. T., & Frank, L. M. (2021). Hippocampal replay of experience at real-world speeds. eLife, 10, e64505.

141. Denovellis, E. L., Frank, L. M., & Eden, U. T. (2019). Characterizing hippocampal replay using hybrid point process state space models. In 53rd Asilomar Conference on Signals, Systems, and Computers (pp. 245-249). Pacific Grove, CA, USA.

142. Navas-Olive, A., Rubio, A., Abbaspoor, S., Hoffman, K. L., & de la Prida, L. M. (2023). A machine learning toolbox for the analysis of sharp-wave ripples reveal common features across species. bioRxiv.

143. Tingley, D., & Peyrache, A. (2020). On the methods for reactivation and replay analysis. Philosophical Transactions of the Royal Society B: Biological Sciences, 375(1799), 20190231.

144. Ambrose, R. E., & Foster, D. J. (2016). Reverse replay of hippocampal place cells is uniquely modulated by changing reward. Neuron, 91, 1124-1136.

145. Wu, C. T., Haggerty, D., Kemere, C., & Ji, D. (2017). Hippocampal awake replay in fear memory retrieval. Nature Neuroscience, 20(4), 571-580.

146. Chenani, A., Sabariego, M., Schlesiger, M. I., Leutgeb, J. K., Leutgeb, S., & Leibold, C. (2019). Hippocampal CA1 replay becomes less prominent but more rigid without inputs from medial entorhinal cortex. Nature Communications, 10(1), 1341.

147. Takahashi, S. (2015). Episodic-like memory trace in awake replay of hippocampal place cell activity sequences. eLife, 4, e08105.

148. Eichenbaum, H. (2013). Memory on time. Trends in Cognitive Sciences, 17(2), 81-88.

149. Knierim, J. J., Neunuebel, J. P., & Deshmukh, S. S. (2013). Functional correlates of the lateral and medial entorhinal cortex: Objects, path integration and local-global reference frames. Philosophical Transactions of the Royal Society B: Biological Sciences, 369(1635), 20130369.

150. Zhang, X. M., & Zhu, J. (2011). Kainic acid-induced neurotoxicity: Targeting glial responses and glia-derived cytokines. Current Neuropharmacology, 9(2), 388-398.

151. Brown, E. N., Frank, L. M., Tang, D., Quirk, M. C., & Wilson, M. A. (1998). A statistical paradigm for neural spike train decoding applied to position prediction from ensemble firing patterns of rat hippocampal place cells. Journal of Neuroscience, 18, 7411-7425.

152. Cruzado, N. A., Tiganj, Z., Brincat, S. L., Miller, E. K., & Howard, M. W. (2020). Conjunctive representation of what and when in monkey hippocampus and lateral prefrontal cortex during an associative memory task. Hippocampus, 30(12), 1332-1346.

153. Shahbaba, B., Li, L., Agostinelli, F., et al. (2022). Hippocampal ensembles represent sequential relationships among an extended sequence of nonspatial events. Nature Communications, 13, 787.

154. Wikenheiser, A. M., & Redish, A. D. (2015). Hippocampal theta sequences reflect current goals. Nature Neuroscience, 18, 289-294.

155. Sosa, M., Plitt, M. H., & Giocomo, L. M. (2024). Hippocampal sequences span experience relative to rewards. bioRxiv.

156. Barron, H. C., Reeve, H. M., Koolschijn, R. S., Perestenko, P. V., Shpektor, A., Nili, H., Rothaermel, R., Campo-Urriza, N., O'Reilly, J. X., Bannerman, D. M., Behrens, T. E. J., & Dupret, D. (2020). Neuronal computation underlying inferential reasoning in humans and mice. Cell, 183(1), 228-243.e21.

157. Whittington, J. C. R., Muller, T. H., Mark, S., Chen, G., Barry, C., Burgess, N., & Behrens, T. E. J. (2020). The Tolman-Eichenbaum Machine: Unifying space and relational memory through generalization in the hippocampal formation. Cell, 183(5), 1249-1263.e23.

158. Whittington, J. C. R., McCaffary, D., Bakermans, J. J. W., & Behrens, T. E. J. (2022). How to build a cognitive map. Nature Neuroscience, 25(10), 1257-1272.

159. McNamee, D. C., Stachenfeld, K. L., Botvinick, M. M., & Gershman, S. J. (2021). Flexible modulation of sequence generation in the entorhinal-hippocampal system. Nature Neuroscience, 24(6), 851-862.

160. George, D., Rikhye, R. V., Gothoskar, N., Guntupalli, J. S., Dedieu, A., & Lázaro-Gredilla, M. (2021). Clone-structured graph representations enable flexible learning and vicarious evaluation of cognitive maps. Nature Communications, 12(1), 2392.

161. Gattas, S., Elias, G. A., Janecek, J., Yassa, M. A., & Fortin, N. J. (2022). Proximal CA1 20-40 Hz power dynamics reflect trial-specific information processing supporting nonspatial sequence memory. eLife, 11, e55528.

162. Grosmark, A. D., & Buzsáki, G. (2016). Diversity in neural firing dynamics supports both rigid and learned hippocampal sequences. Science, 351(6277), 1440-1444.

163. Wu, X., & Foster, D. J. (2014). Hippocampal replay captures the unique topological structure of a novel environment. Journal of Neuroscience, 34(18), 6459-6469.

164. Michon, F., Sun, J. J., Kim, C. Y., Ciliberti, D., & Kloosterman, F. (2019). Post-learning hippocampal replay selectively reinforces spatial memory for highly rewarded locations. Current Biology, 29(9), 1436-1444.